AD-A081 127 WYOMING UNIV LARAMIE DEPT OF ATMOSPHERIC SCIENCE F/G 4/1
CONDUCT OF CLOUD SPECTRA MEASUREMENTS.(U)
OCT 79 G VALI, M K POLITOVICH F19628-79-C-0029
UNCLASSIFIED SCIENTIFIC-1 AFGL-TR-79-0251 NL

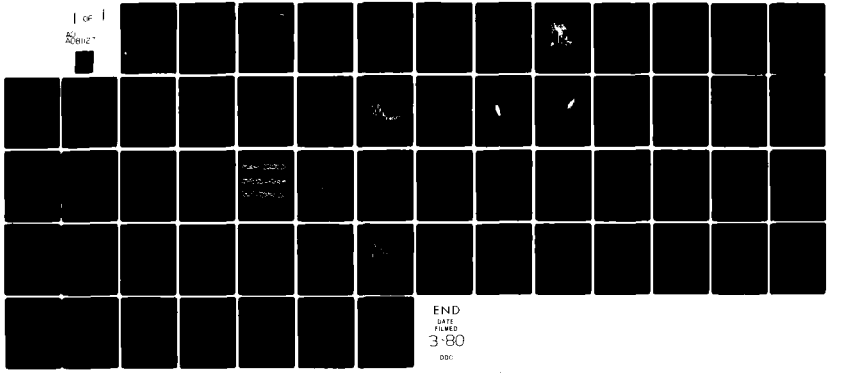

END
DATE FILMED
3-80
DDC

AFGL-TR-79-0251

CONDUCT OF CLOUD SPECTRA MEASUREMENTS

Gabor Vali
Marcia K. Politovich
Darrel G. Baumgardner
William A. Cooper

University of Wyoming
Department of Atmospheric Science
P.O. Box 3038
Laramie, Wyoming 82071

Scientific Report No. 1

Date of Report 12 October 1979

Approved for public release; distribution unlimited

AIR FORCE GEOPHYSICS LABORATORY
AIR FORCE SYSTEMS COMMAND
UNITED STATES AIR FORCE
HANSCOM AFB, MASSACHUSETTS 01731

Unclassified

SECURITY CLASSIFICATION OF THIS PAGE (When Data Entered)

REPORT DOCUMENTATION PAGE

READ INSTRUCTIONS BEFORE COMPLETING FORM

1. REPORT NUMBER: AFGL-TR-79-0251	2. GOVT ACCESSION NO.
3. RECIPIENT'S CATALOG NUMBER: Rept. for	
4. TITLE (and Subtitle): CONDUCT OF CLOUD SPECTRA MEASUREMENTS.	5. TYPE OF REPORT & PERIOD COVERED: Scientific Report 1 Dec 78 — 30 Sep 79
	6. PERFORMING ORG. REPORT NUMBER
7. AUTHOR(s): Gabor Vali, Marcia K. Politovich, Darrel G. Baumgardner, William A. Cooper	8. CONTRACT OR GRANT NUMBER(s): F19628-79-C-0029
9. PERFORMING ORGANIZATION NAME AND ADDRESS: University of Wyoming, Dept. of Atmospheric Science, P.O. Box 3038, Laramie, Wyoming 82071	10. PROGRAM ELEMENT, PROJECT, TASK AREA & WORK UNIT NUMBERS: 62101F, 6670[illegible]AA, 12
11. CONTROLLING OFFICE NAME AND ADDRESS: Air Force Geophysics Laboratory, Hanscom AFB, Massachusetts 01731, Monitor/Rosemary M. Dyer/LY	12. REPORT DATE: 12 Oct 1979
	13. NUMBER OF PAGES: 60
14. MONITORING AGENCY NAME & ADDRESS (if different from Controlling Office)	15. SECURITY CLASS. (of this report): Unclassified
	15a. DECLASSIFICATION DOWNGRADING SCHEDULE

16. DISTRIBUTION STATEMENT (of this Report)

Approved for public release; distribution unlimited.

17. DISTRIBUTION STATEMENT (of the abstract entered in Block 20, if different from Report)

18. SUPPLEMENTARY NOTES

19. KEY WORDS (Continue on reverse side if necessary and identify by block number)

Cloud Spectra Measurements
Cloud Particle Concentrations

20. ABSTRACT (Continue on reverse side if necessary and identify by block number)

Reasons for instrumental errors in cloud particle spectra measurements were investigated. Calibrations and tests on four probes manufactured by Particle Measuring Systems, Inc. (PMS) were conducted in the laboratory and in a wind tunnel at the University of Wyoming's Elk Mountain Observatory.

Bench determinations of the sample area of the ASSP found it to be 0.35 mm^2 compared with PMS's value of 0.32 mm^2, and the velocity reject precentage was found to be 68% compared to 62%. Strong correlations were found between ASSP

DD FORM 1 JAN 73 1473 EDITION OF 1 NOV 65 IS OBSOLETE

404271

Unclassified

SECURITY CLASSIFICATION OF THIS PAGE (When Data Entered)

and FSSP measurements; however, there was a factor of three difference between the FSSP and ASSP droplet concentrations which may have been due to a malfunction of the FSSP. Comparisons of ASSP and soot impaction slide data showed good agreement for measured droplet size, but a sampling problem with the cloud gun may have resulted in excessively high concentrations.

The 2D-C probe response was found to be in close agreement with PMS specifications for particles > 100 μm. For the lower size channels the counting efficiencies were determined to be higher than indicated by PMS but these results could also have resulted from the missizing of larger particles.

The 1D-C probe undercounted particles in the lower channels ($\lesssim$ 140 μm) due to the reduced depths of field for these channels. Revised depths of field ranged from 3.23 μm for the first channel (compared to 1.45 given by PMS) to 92.72 mm for the eighth channel (compared to 61.00 mm), with decreasing values for higher channels. The measured diameters of particles increased as the particles were detected further from the focal plane of the laser beam. This resulted in slight oversizing of the particles by about 25% near 100 μm and decreasing to < 10 % near 250 μm.

The FSSP and ASSP probes responded to ice particles with a nearly uniform distribution of counts in all channels. These counts yielded concentrations of ice particles 2 1/2 - 3 1/2 orders of magnitude higher than those actually present.

Suggestions for further investigation into cloud particle spectra measurments are listed at the end of the report.

TABLE OF CONTENTS

1. Introduction - 1
2. Instruments used in Tests - 1
   a. Particle Measuring Systems (PMS) Axially Scattering Spectrometer Probe (ASSP)- 1
   b. PMS Forward Scattering Spectrometer Probe (FSSP) - - - - - - - - - 1
   c. PMS Optical Array Cloud Droplet Spectrometer Probe (1D-C)- - - - 2
   d. PMS 2D Optical Array Spectrometer Probe (2D-C) - - - - - - - - - - 2
3. Procedure - 2
4. Results and Discussion - 2
   a. Sample area studies using the ASSP - - - - - - - - - - - - - - - - 2
   b. ASSP and cloud gun slide intercomparison - - - - - - - - - - - - - 7
   c. ASSP-FSSP comparisons -15
   d. Studies of the 2D-C probe response - - - - - - - - - - - - - - - -21
   e. Studies of the 1D-C probe response - - - - - - - - - - - - - - - -29
   f. Study of the response of the ASSP and FSSP to ice particles - -43

5. Summary and Conclusions- -54

References 56

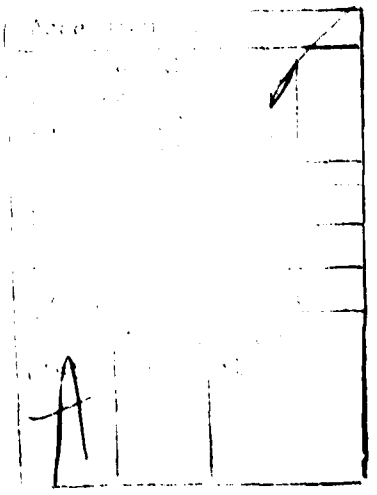

Axially Scattering Spectrometer Probe (ASSP and Forward Scattering Spectrometer Probe (FSSP)

1. Introduction

The work to be reported here addressed the following objectives: (as detailed in the Technical Proposal):

1. Compare bench determinations of ASSP and FSSP sample areas with determinations during actual cloud sampling;

2. Evaluate the accuracy of the overlap in size range between FSSP and ID-C probes;

3. Evaluate the response of the ASSP and FSSP probes to ice crystals;

4. Check the statistical correction schemes used to deal with ID-C counts in the lowest and highest size categories.

The information needed to accomplish these objectives was collected by performing special tests with the probes in question. These tests were conducted, for the most part, at the Elk Mountain Laboratory, during times when the Observatory was enveloped by clouds. Bench and wind-tunnel tests were utilized. In addition, data were derived from aircraft penetrations of clouds, with identical probes as those used at the Observatory.

The tests have yielded some important new insights on the questions formulated in the objectives. These results should be helpful to interpretations of data collected by AFGL and other research aircraft PMS probes. However, as is the nature of research, the results also revealed additional questions and yet unexplainable features, so that it appears fruitful to pursue the evaluations further.

2. Instruments used in tests

a. Particle Measuring Systems (PMS) Axially Scattering Spectrometer Probe (ASSP)

Model: ASSP - 100

History: This unit is on loan to us by the Bureau of Reclamation. The unit was refurbished by PMS during the summer of 1978. "Strobe' and "Activity" circuitry was added in October 1978.

b. PMS Forward Scattering Spectrometer Probe (FSSP)

Model: FSSP-100

Serial No: 80-5T-7607-1980

History: This unit was leased from PMS for the duration of the tests. The unit has been used by PMS as a reference standard.

c. PMS Optical Array Cloud Droplet Spectrometer Probe (1D-C)

Model: OAP - 200X

Serial No.: 735-0678-09

History: This unit was leased from PMS for the duration of the tests. It had been calibrated at PMS to 20 μm channel widths on 7 March 1979.

d. PMS 2D Optical Array Spectrometer Probe (2D-C)

Model: OAP - 2D-C

Serial No.: 393-0377-01A

History: This unit was leased from PMS for the duration of the tests.

3. Procedure

The majority of the studies here reported were performed at the Elk Mountain Observatory. A slow-speed (25 ms^{-1}) wind tunnel was utilized; two probes at a time could be installed in the wind tunnel. The wind tunnel and the instrument platform on which supplementary measurements were taken are shown in Figure 1.

Data collection was performed primarily during periods of time when the Observatory was enveloped by clouds. Additional data were obtained by generating large numbers of small ice crystals near the entrance of the wind tunnel with a spray of liquified propane.

The data processing and recording systems were located inside the Observatory.

Table 1 summarizes the periods of field observations.

4. Results and Discussion

a. Sample area studies using the ASSP

With the ASSP mounted on the bench, the electronic depth of field was first determined with the method given by PMS. This procedure involved placing oscilloscope probes on the amplifier outputs from the signal and annulus photodetectors before they are capacitively decoupled. A translucent material is then passed from one extreme of the beam to the other, noting the two points where the signal voltage crosses the annulus voltage. These two points determined the actual depth of field to be 4.0-4.2 mm. By projecting the beam at a right angle onto a scale, the beam width was determined to be 0.18 mm. The depth of field and beam

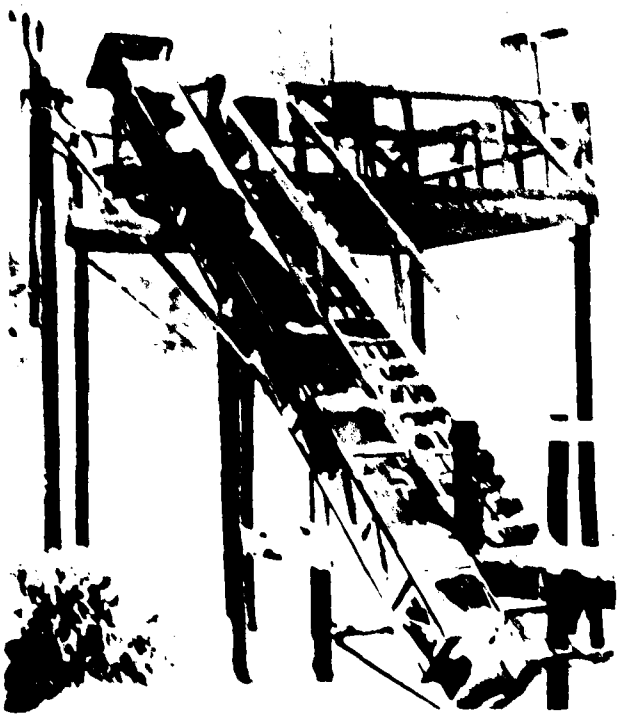

Figure 1 Wind tunnel attached to instrument platform at the Elk Mountain Observatory. ASSP, FSSP, 1D-C and 2D-C probes were installed one-fourth of the way up from the axial fan blower at the bottom of the tunnel.

TABLE 1 1978-79 SUMMARY
OF FIELD TEST PERIODS

DATE	ASSP	FSSP	1D-C	2D-C	COMMENTS
12 Mar 79					Installation of instruments
13 Mar 79	✓			✓	Study of effect of ice particles on ASSP spectrum
16 Mar 79	✓		✓		Comparison of ASSP - 1D-C in overlap region
12 Mar 79			✓	✓	Small ice particle studies
25 Mar 79	✓	✓			ASSP-FSSP intercomparison
			✓	✓	Small ice particle studies
	✓		✓		Comparison of ASSP-1D-C in overlap region
			✓		Glass bead calibrations in lab using mobile aperture
2 Apr 79				✓	Glass bead calibration in lab using mobile aperture
			✓	✓	Small ice particle studies
			✓	✓	Mobile aperture affixed to 2D-C
3 Apr 79			✓	✓	Mobile aperture affixed to 2D-C
			✓	✓	Mobile aperture affixed to 1D-C
		✓		✓	Study of effect of ice on FSSP specturm
			✓	✓	Small ice particle studies
4 Apr 79	✓		✓		Comparison of ASSP - 1D-C in overlap region

KEY: ASSP - PMS axially Scattering Spectrometer Probe
FSSP - DMS Forward Scattering Spectrometer Probe
1D-C - PMS 1D Optical Array Spectrometer Probe
2D-C - PMS 2D Optical Array Spectrometer Probe

diameter measured agreed favorably with those specified by PMS when we received the instrument (4.0 mm and 0.18 mm, respectively). Although the beam diameter and depth of field determine the total sample area, the effective sample area is smaller due to the velocity rejection circuitry which is used to minimize edge effect errors. This mechanism gives an effective sample area 62% of the total area according to the PMS data. The accuracy of this value was tested while the ASSP was on the bench according to the following procedure.

An aluminum tube, fitted with glass windows, was fabricated to fit in the throat of the ASSP. A movable brass slide was inserted just far enough to be secure and yet not have its flattened side in the air stream. The apparatus is shown in Figure 2. After adjusting the tube so that the laser beam of the ASSP passed cleanly through the windows, a vacuum hose was attached to the tube and air was drawn through at an approximate rate of 18.5 ms^{-1}. At first 200-300 glass beads, 10-15 μm in diameter, were passed through the tube to establish a steady velocity average. The brass slide was then pushed completely into the calibration tube until snug and 400-500 more beads were passed through the tube. After totaling the counts seen by the ASSP, the brass slide was removed and placed under the microscope where the glass beads which stuck to the silicone coated surface were counted over a representative area. The effective sample area was determined from the ratio of concentrations and the sampling on the slide by the formula:

$$ESA = NA*SA/NS$$

Where: ESA = Effective Sampling Area
NA = Total counts seen by ASSP
NS = Total counts over slide area
SA = Slide Area over which beads were counted.

Using an average over several runs, the effective sample area was found to be within 10% of that determined by PMS, with our value shown to be 0.35 mm^2 while the PMS value was stated to be 0.32 mm^2. The velocity rejection percentage is thus higher (68%) than the original specifications state (62%).

This calibration technique has been utilized on several occasions and was found to be an effective method of checking the sampling area of the ASSP from time to time.

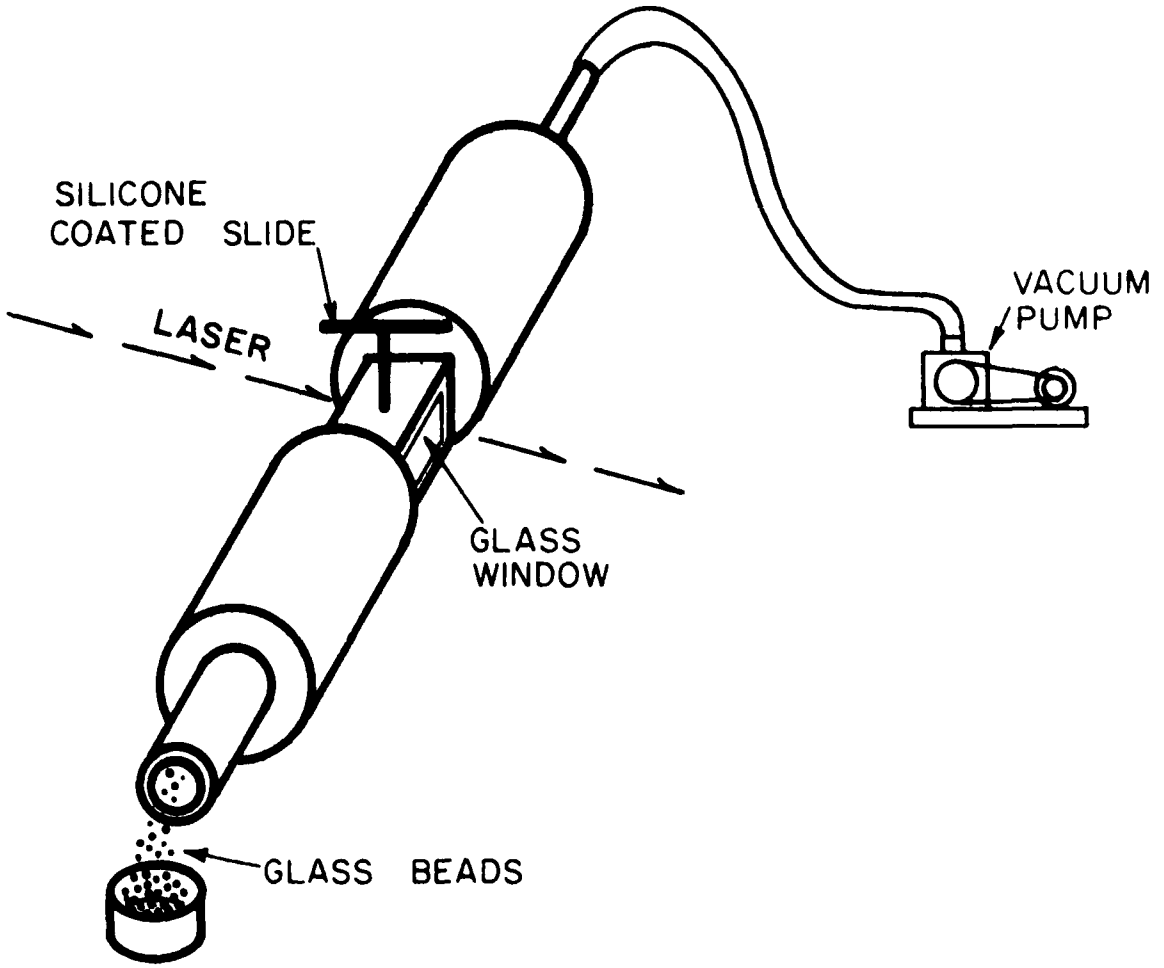

ASSP CALIBRATION TUBE

Figure 2 The ASSP Calibration Tube used in the Studies.

b. ASSP and cloud gun slide intercomparison

A total of 63 soot-coated plastic slides (CGS) were exposed for droplet impaction during the 1978-79 field season at Elk Mountain. Forty-one of these slides were compared with ASSP data recorded during the same periods of time. The remainder of the slides were eliminated from the comparisons due to occasional failure of the cloud gun mechanism, ASSP icing in the wind tunnel, or defective soot coatings.

After sizing the craters in the soot and deriving the corresponding droplet diameters, the data was stored in the computer and a number of graphical analyses were conducted. Figure 3 shows a typical spectral comparison as measured by the cloud gun and ASSP. The first things which may be noted are the differences in spectral width and concentrations. The broadening of the spectrum by the ASSP has been also documented previously (Walsh, 1977). The difference in concentrations does appear puzzling in light of aircraft studies which show that typically, for concentrations $\lesssim 500\ cm^{-3}$, the ASSP tends to measure higher concentrations than those seen by the cloud gun. The reason for this discrepancy will be discussed below.

Figures 4 through 7 show the comparisons between ASSP and CGS concentrations, mean diameters, standard deviations of the mean diameters and liquid water contents. Figure 8 shows a portion of an ASSP record averaged over 10 s intervals for $\sim$3 hours, with the corresponding CGS values. It is obvious from this graph that the cloud parameters can vary sharply over relatively short periods of time. This is not explained by differences in sampled volume between the ASSP and CGS ($\sim 10\ cm^3$/sec for the continuously recording ASSP; $\sim 12\ cm^3$/sample at 5 ms for the CGS). The difference in position of the two sampling instruments may account for some of the scatter (this will be discussed further below).

During the field season, liquid water was also being measured by a rotating riming rod whose mass accretion rate determined the liquid water content of the air. The sampling time of this device was typically 10-15 min. As seen in Figure 9 the relative variations for the riming rod and the ASSP appear to be a good agreement but the absolute values are not exactly reconcilable. These data appear to reinforce the credibility of the ASSP while raising some questions as to the validity of some of the data points determined by the CGS.

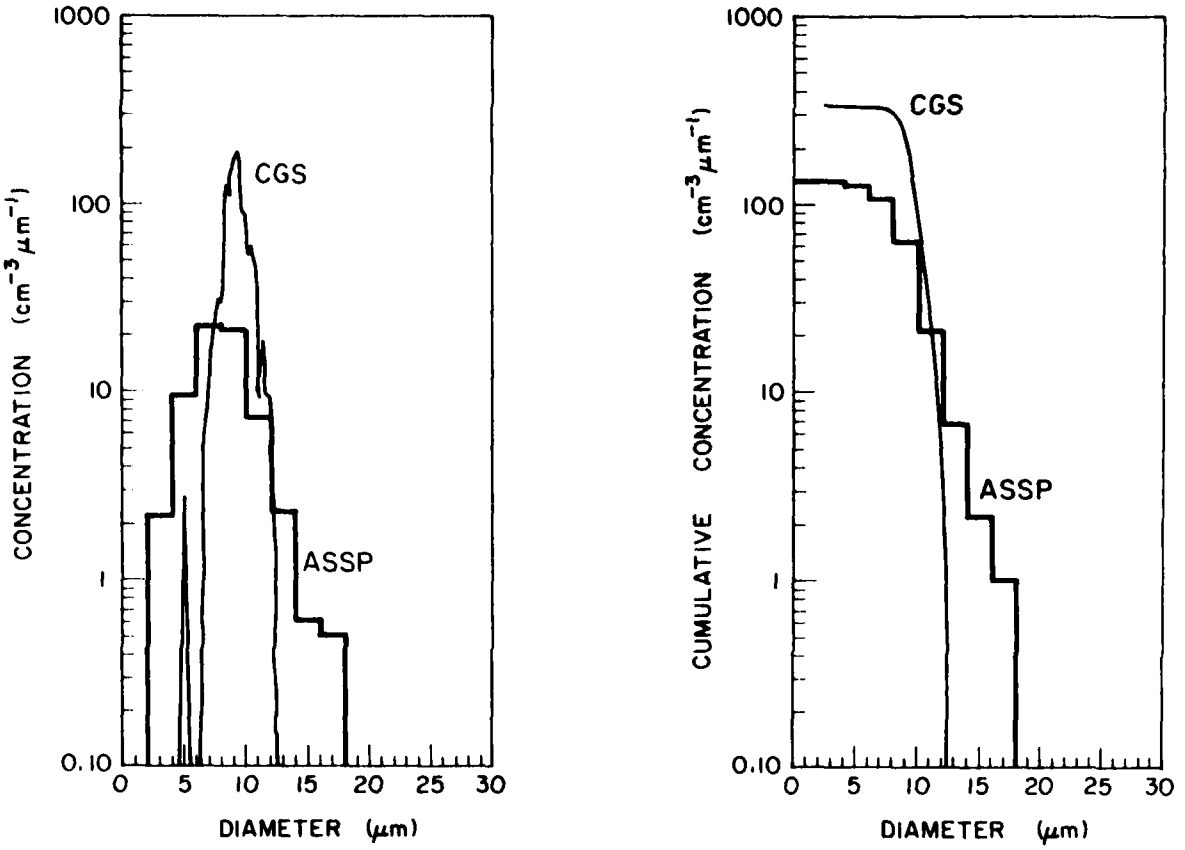

Figure 3 Differential and cumulative concentrations plotted against diameter for cloud droplets sampled by the ASSP and CGS at *155600, 9 January 1979, at the Elk Mountain Observatory.* The ASSP and CGS sampling times were 1 s and 5.8 ms respectively. ASSP droplet concentration was 131.4 cm^{-3}, the corresponding CGS value was 334.9 cm^{-3}.

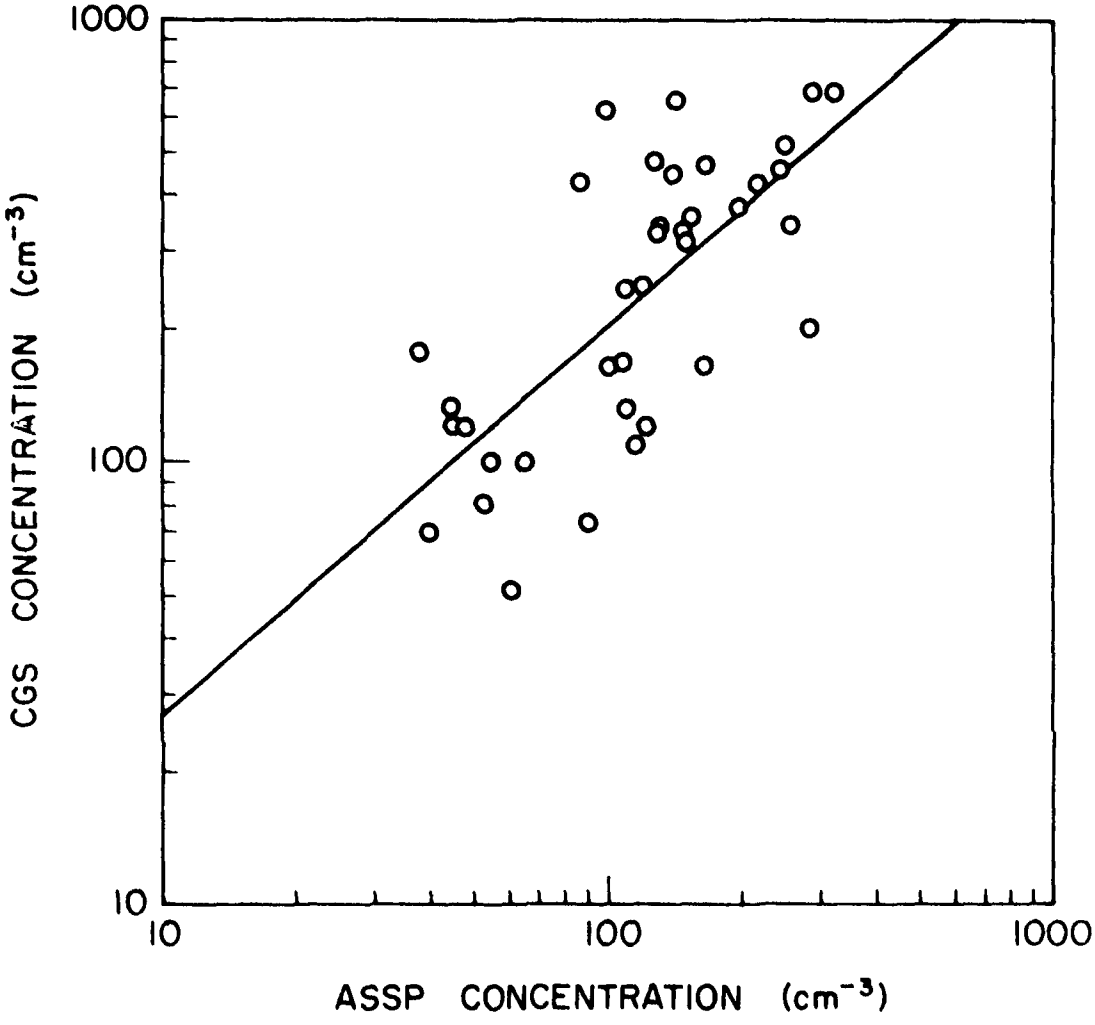

Figure 4 CGS versus ASSP-measured droplet concentration (N) from 37 samples taken from 9 January - 4 April 1979 at the Elk Mountain Observatory. Best fit using a least-squares method is represented by a line described by $N_{cgs} = 3.60\ N_{assp}^{0.88}$, with a correlation coefficient of 0.71.

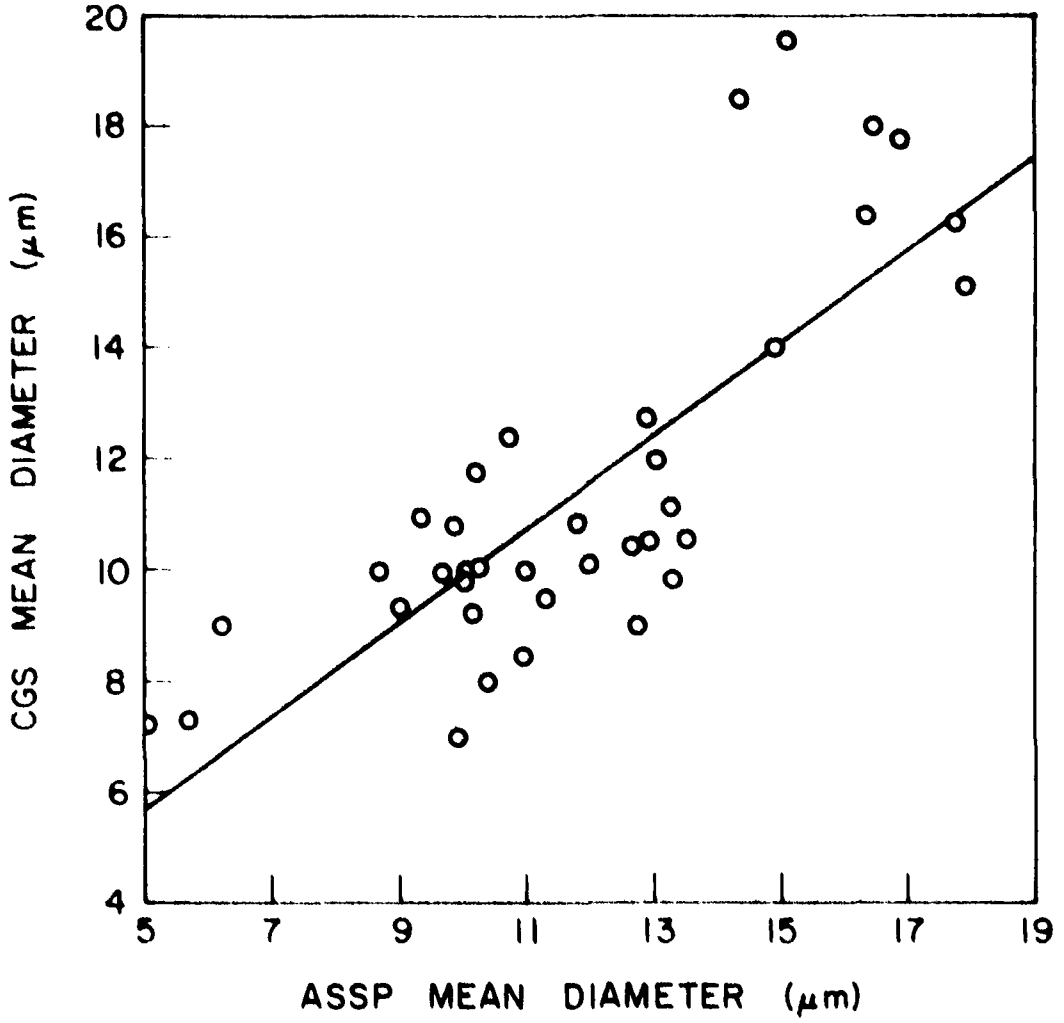

Figure 5. CGS versus ASSP-measured mean diameters ($\bar{d}$) from the same set of data shown in Figure 4. Best fit to the data is represented by a line described by $\bar{d}_{cgs} = 0.84\ \bar{d}_{assp} + 1.46$, with a correlation coefficient of 0.79.

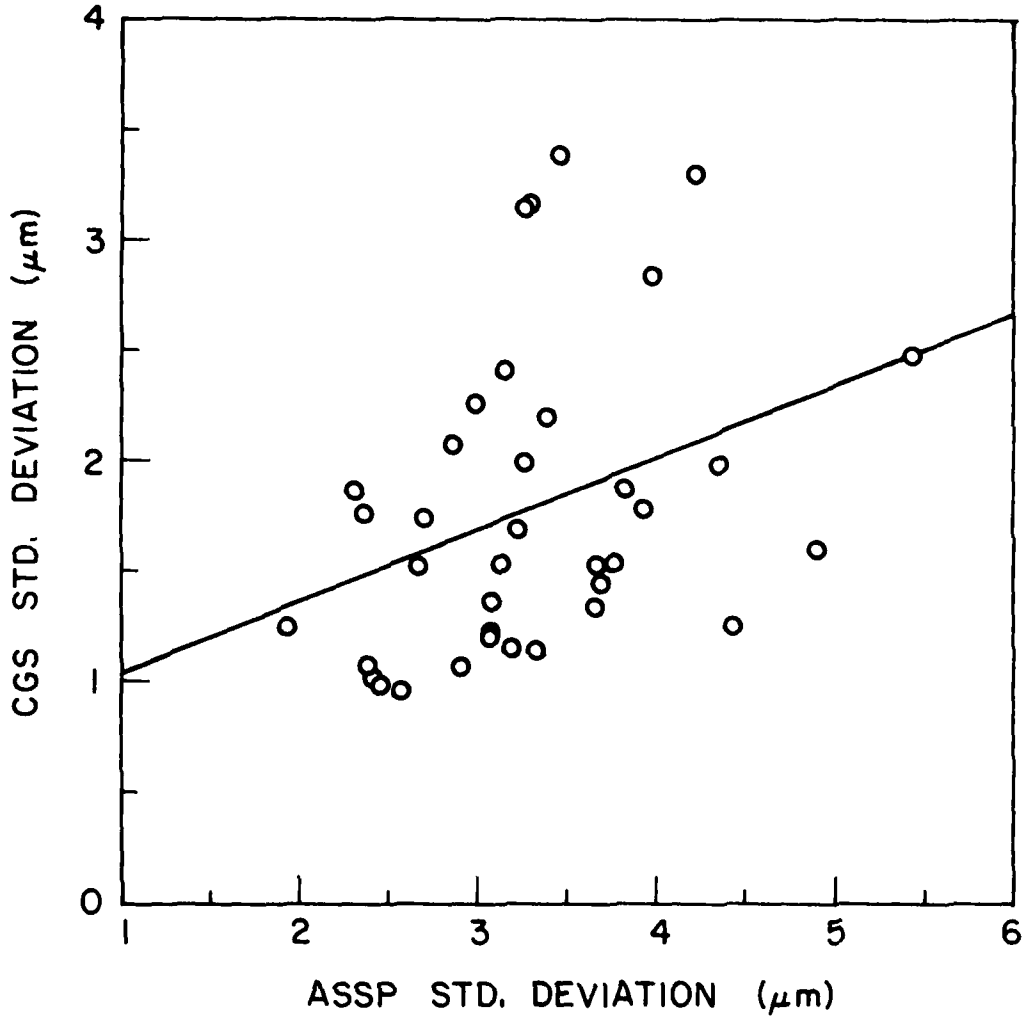

Figure 6 CGS versus ASSP-measured standard deviation (σ) of the mean diameter for the sample set shown in Figures 4 and 5. Best fit to the data is represented by a line described by

$\sigma_{cgs} = 0.32\sigma_{assp} = 0.71$, with a correlation coefficient of 0.35.

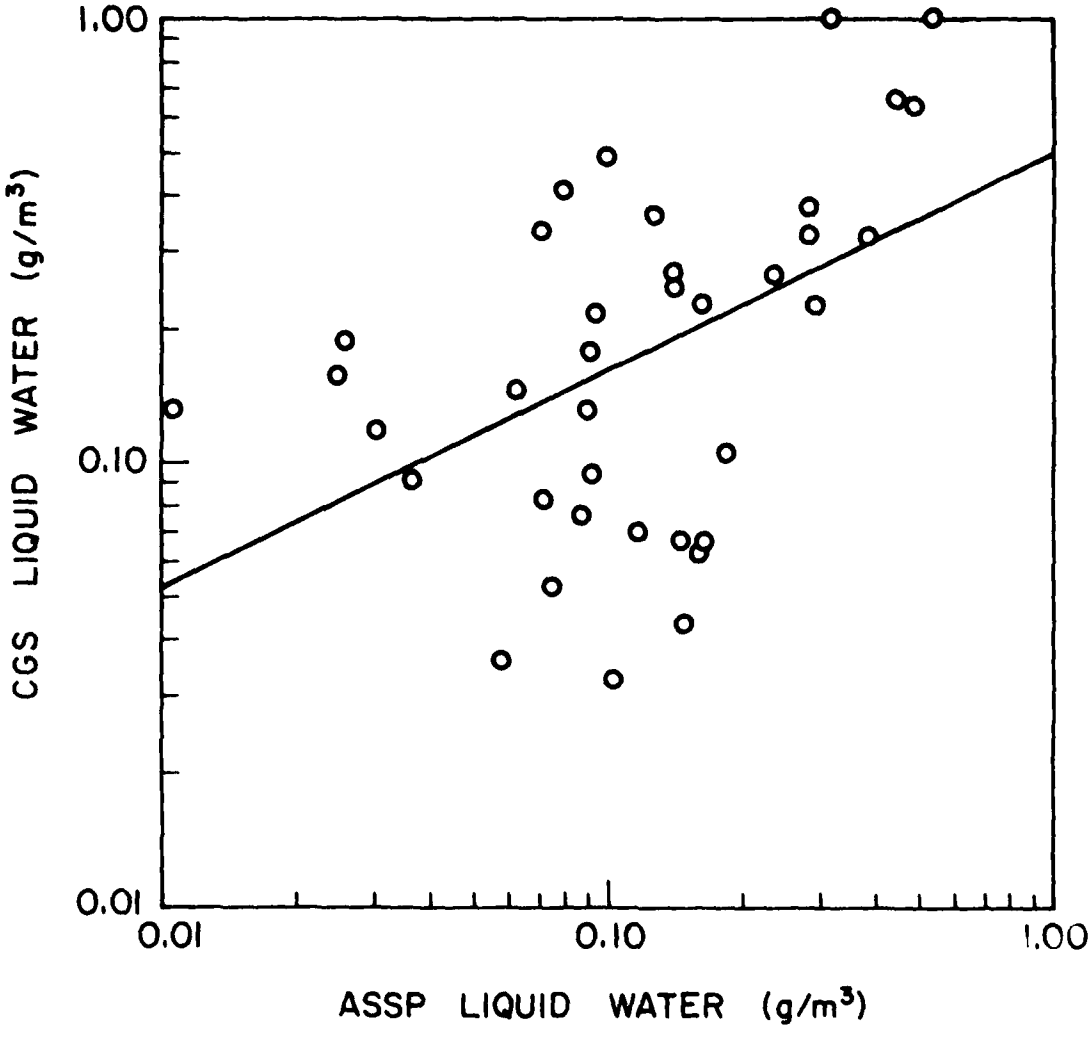

Figure 7 CGS versus ASSP-measured liquid water contents (LWC) for sample set shown in Figures 4-6. Best fit to the data is represented by a line described by $LWC_{cgs} = 0.50\ LWC_{assp}^{0.49}$, with a correlation coefficient of 0.46.

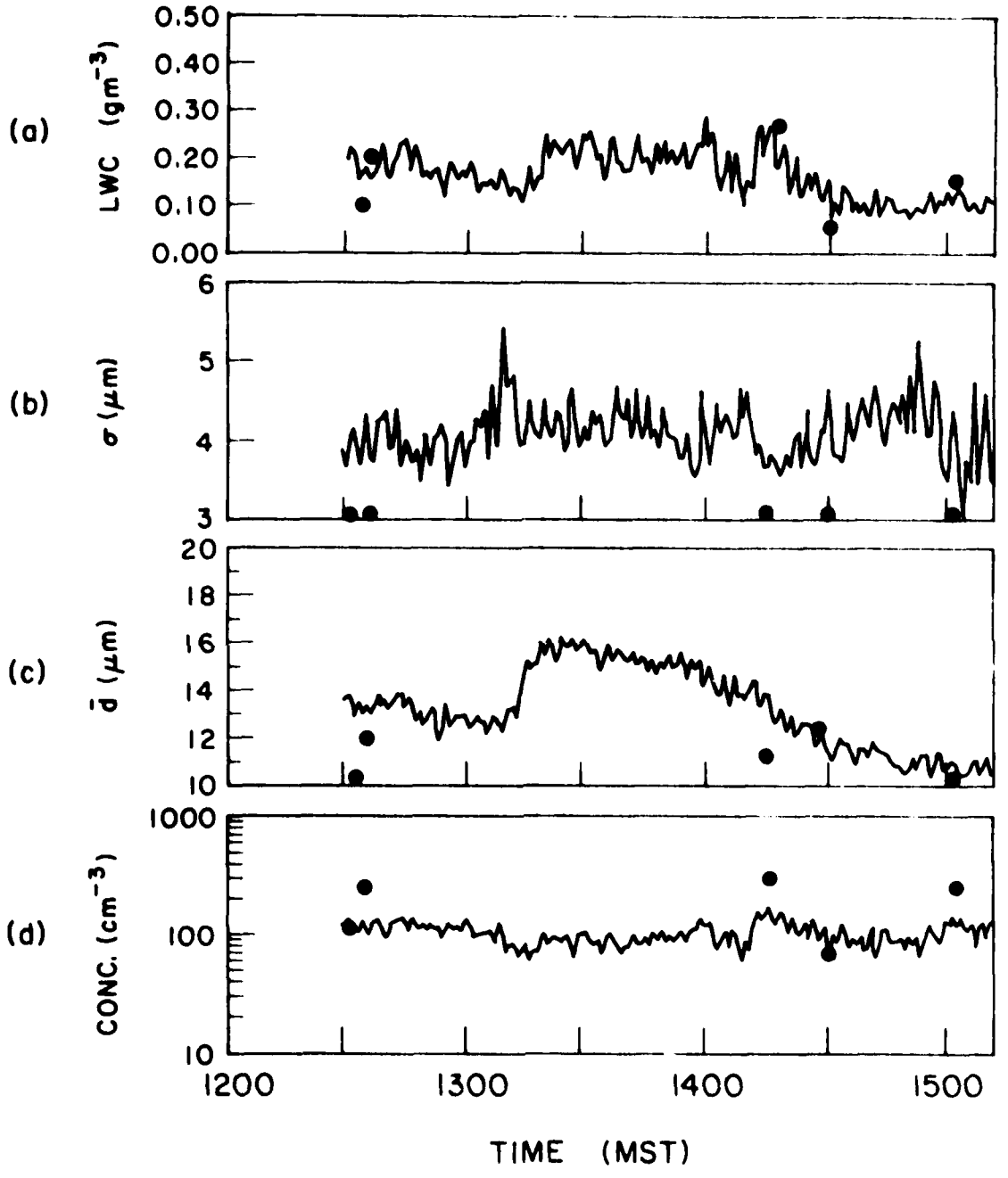

Figure 8 Variation with time of ASSP-measured parameters from 1230 to 1515 on 10 Jan 1979. (a) Liquid water content, (b) standard deviation of the mean diameter, (c) mean diameter and (d) droplet concentration. A 60 s averaging period was used to "smooth out" the data. CGS values of the parameters are also indicated (●).

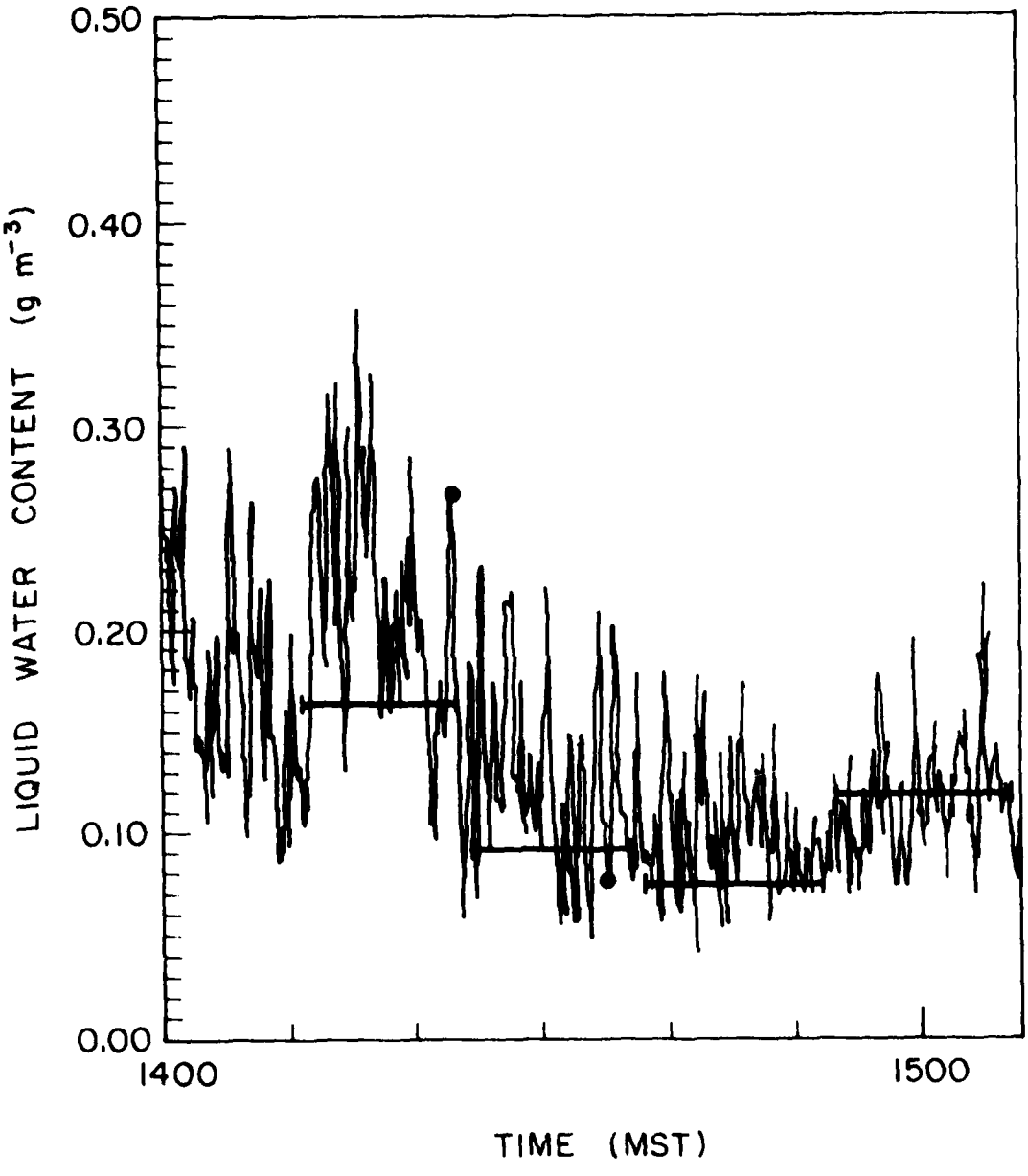

Figure 9 Variation with time of liquid water content measured by the ASSP (_____), riming rod (⟝⟞) and cloud gun slides (●). Samples were taken from 1400 - 1510 MST on 10 Jan 1979.

The concentrations as measured by the UGS were typically a factor of 2-3 greater than those measured by the ASSP. The first explanation for this discrepancy appeared to be that there were losses in the wind tunnel due to turbulence. After the comparison with riming rod data, the ASSP now appears to be more accurately measuring the concentrations. The cloud gun currently being used at the observatory is an older version of the type now used on our aircraft. Its sampling aperture is bulky, so that due to streamline compression sampling volume might be higher than that which is used in the calculations. The cloud gun is now being modified for the 1979-80 field season to have a sampling cross section duplicating that of the aircraft system. The timing mechanism is also being updated to increase its accuracy; the timing of the exposure time for this past season could not take into account small variations in slide passage time as does the current aircraft system. We anticipate that the discrepancy between the two instruments will be resolved in the coming field season with the changes in geometry and timing and insertion of the cloud gun in the tunnel next to the ASSP rather than at the mouth of the tunnel.

c. ASSP-FSSP Comparisons

The ASSP and FSSP were positioned together in the wind tunnel for a period of about one hour (refer to Table 1). Figures 10 through 12 show scattergrams of 1 s values, relating concentration, mean droplet diameter, and liquid water content as measured by the ASSP and FSSP. Figure 13 shows the average spectral distribution over approximately an hour's duration and Figure 14 shows a portion of the ASSP/FSSP concentrations and liquid water contents over a time period of ~ 2 min. Figure 10 shows a good linear relationship between the concentrations as measured by the two probes, however, the concentrations seen by the ASSP appear to be a factor of three higher than those measured by the FSSP. The mean diameters as shown in Figure 11 show the ASSP sensing larger diameters on the average than the FSSP. The source of this discrepancy becomes obvious when looking at Figure 13 where the FSSP shows much higher concentrations in the lower diameters than does the ASSP. The cause for this negative skewness is not fully understood but a strong possibility is that there was either an internal or external source of noise which was picked up on the lower FSSP channels. This discrepancy will be resolved during the next field season. The liquid watercontent (LWC) as measured by the two instruments is a reflection of the discrepancies between the two instruments in

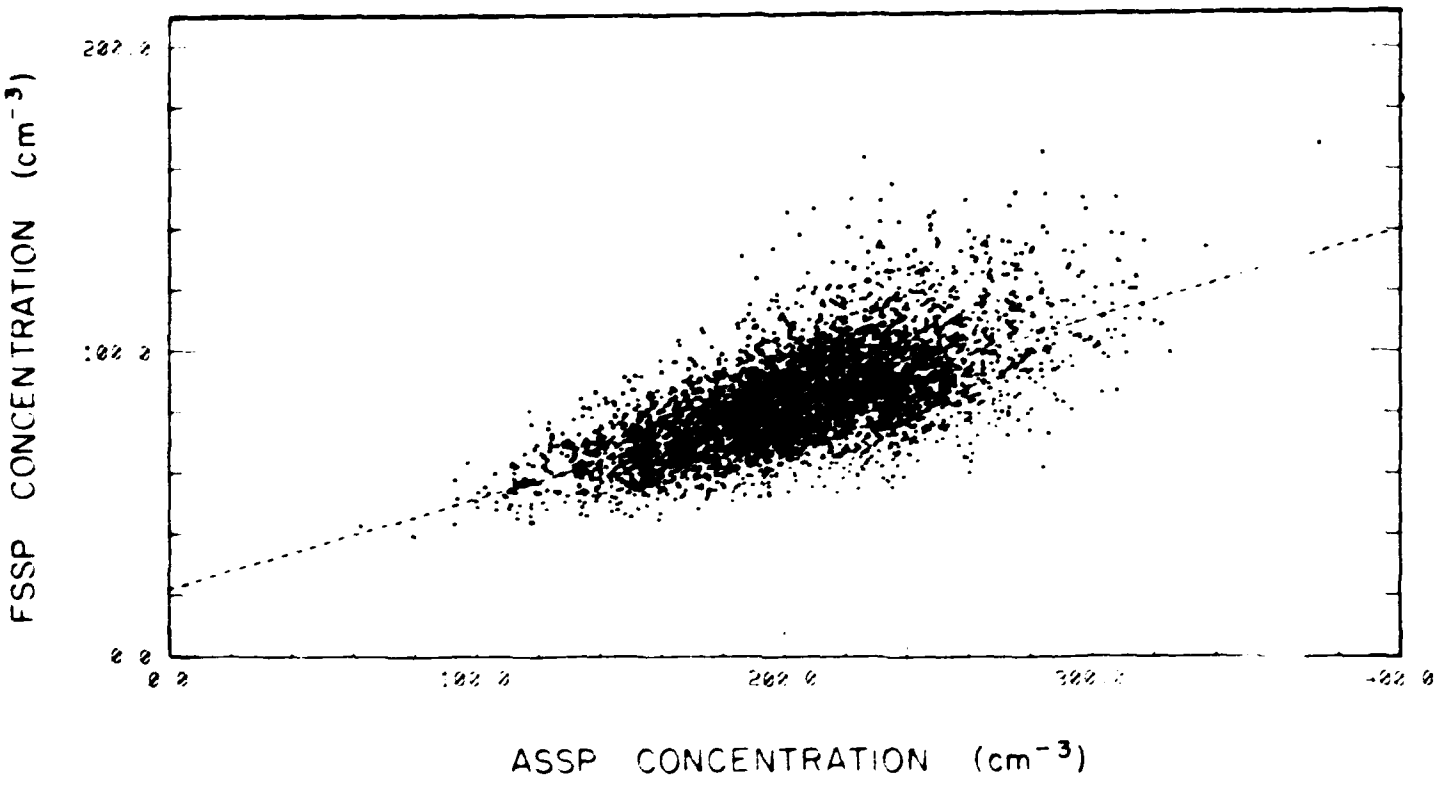

Figure 10. FSSP versus ASSP-measured droplet concentrations from 163545-180345 MST on 25 March 1979. Each data point represents a 1 s average of data. Only those concentrations > 10 cm^{-3} were plotted. The dashed line represents the best-fit line to the 6602 data points (using a least-squares method) described by $N_{fssp} = 0.35\ N_{assp} + 22.3$, with a regression coefficient of 0.67.

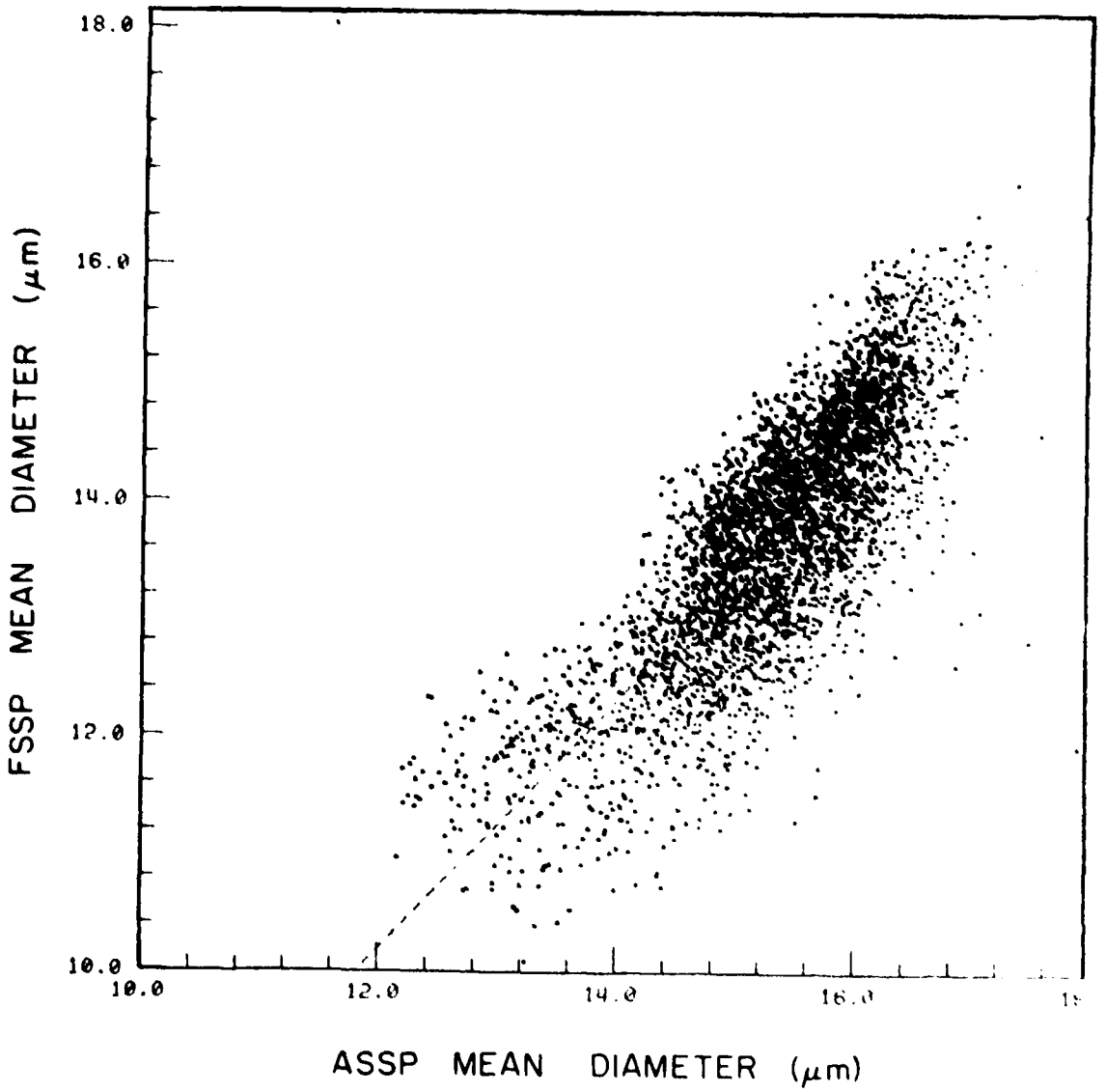

Figure 11 FSSP versus ASSP-measured mean diameters for the sample set presented in Figure 10. The dashed line represents the best fit to the data, described by $\bar{d}_{fssp} = 1.06\ \bar{d}_{assp}^{-2.58}$, with a regression coefficient of 0.80.

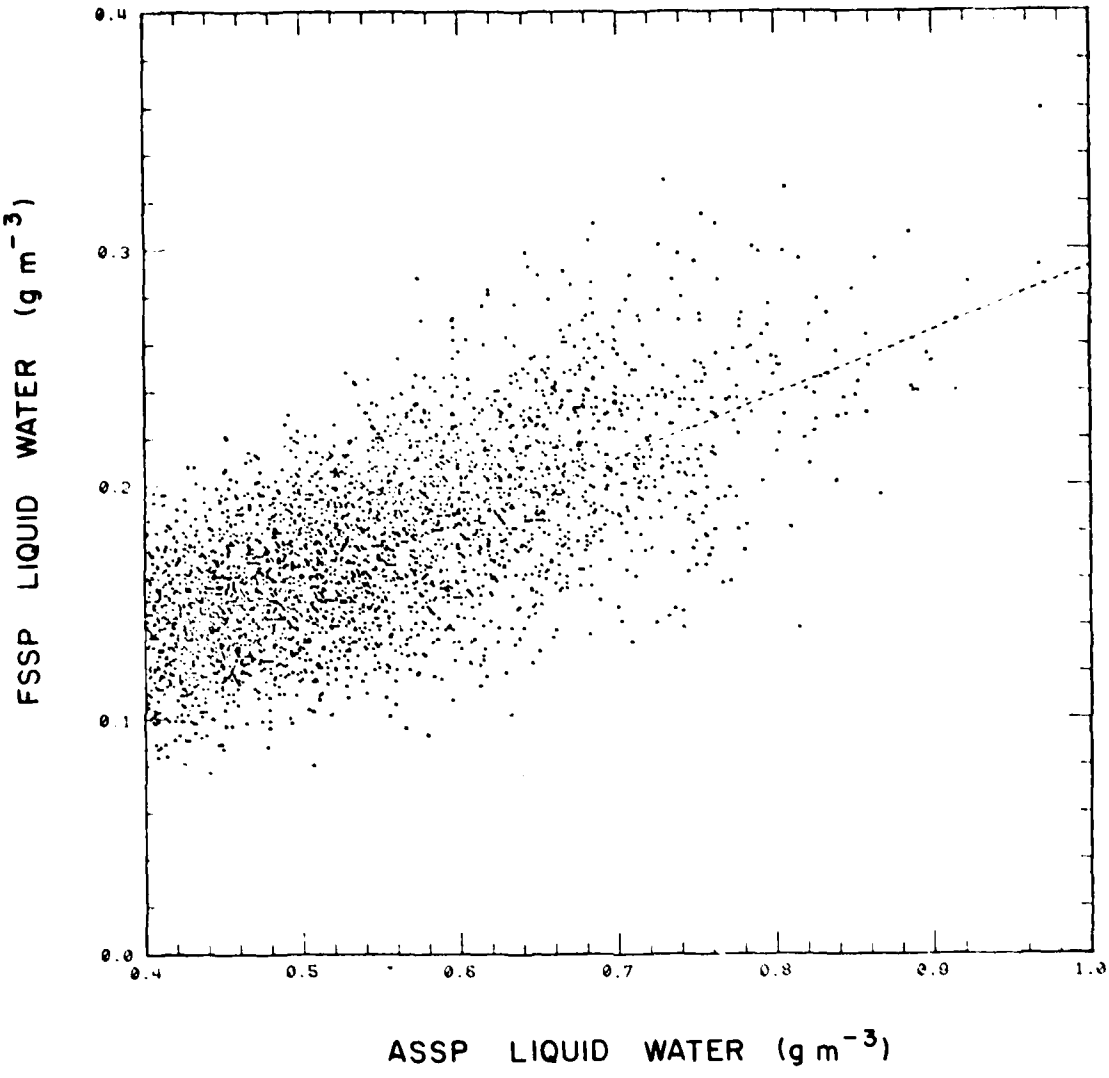

Figure 12 FSSP versus ASSP-measured liquid water contents (LWC) for the data points presented in Figures 10 and 11. The dashed line represents the best fit to the data, described by $LWC_{fssp} = 0.27\ \sigma^{LWC}_{assp} + 0.02$, with a regression coefficient of 0.77.

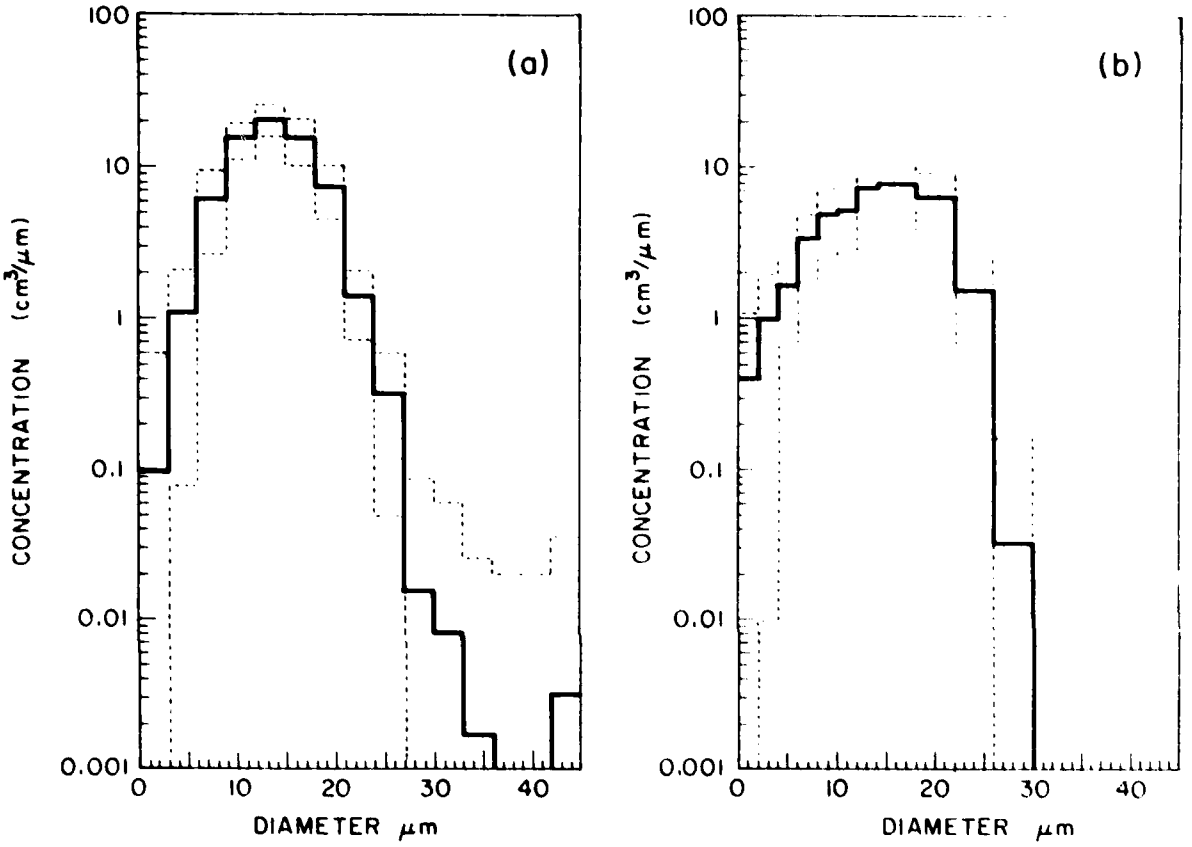

Figure 13 Concentration plotted against diameter measured by the (a) ASSP and (b) FSSP for 25 Mar 1979. Data plotted represents the average (———) and the range within one standard deviation (-----) for data taken from 165345 - 180347 MST.

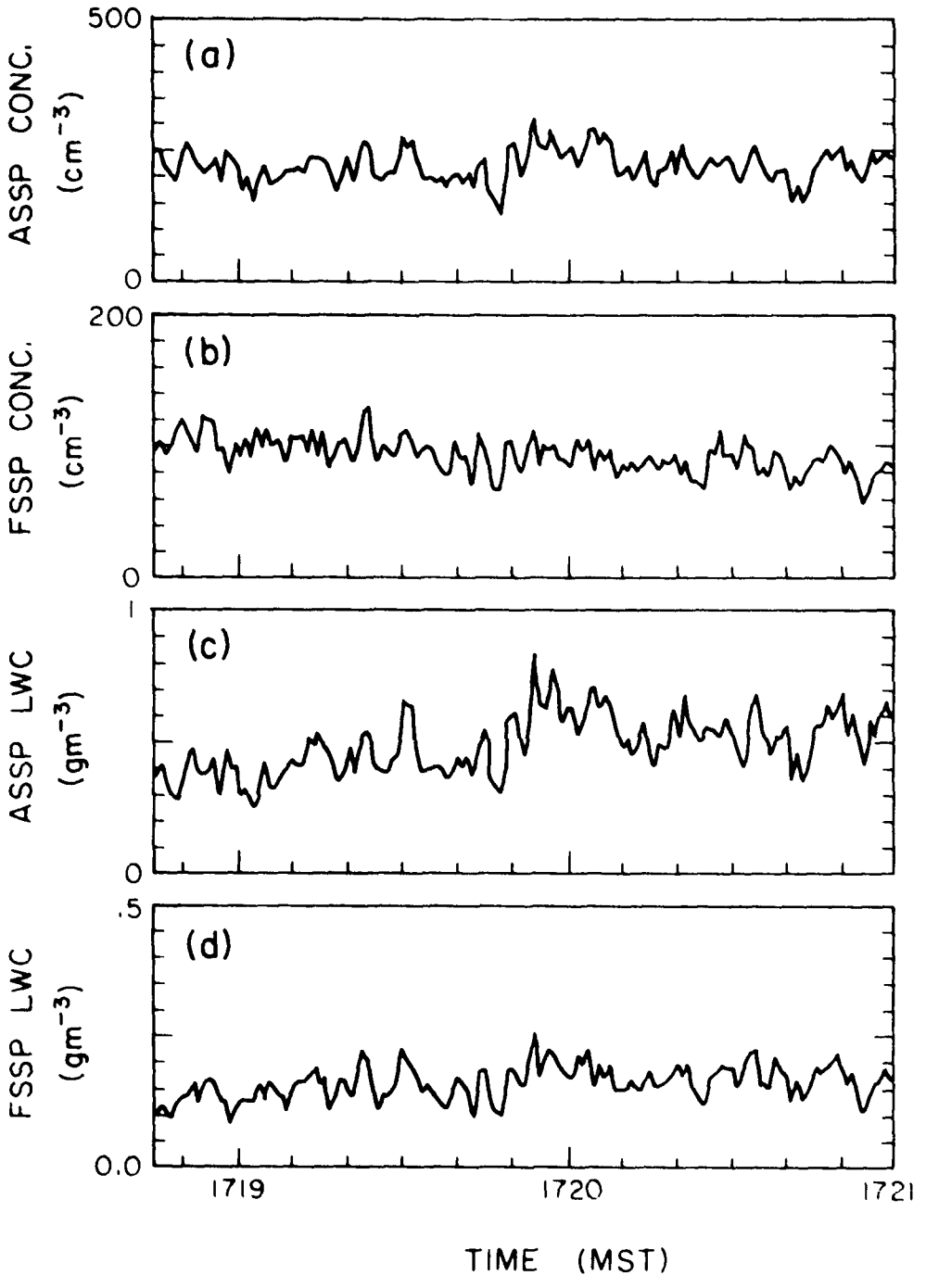

Figure 14 Variation with time of (a) ASSP droplet concentration (b) FSSP droplet concentration (c) ASSP liquid water content and (d) FSSP liquid water content. Data were taken from 171845-172100 on 25 March 1979.

concentration and diameter. The ASSP LWC values are almost a factor of three higher than the FSSP values. Aside from the difference in absolute magnitude, Figure 14 shows that both instruments appear to be responding to the same changes in cloud water and droplet concentration, insuring that the instruments are not just experiencing random fluctuations.

The factor of three differences in concentration remains a puzzle which will remain a point of speculation until the next field season. Possible causes might have been the shifting of the FSSP sample area, or possibly a malfunction of the FSSP. The latter hypothesis is based upon the actual failure of the FSSP near the end of the field season. The real answer will remain unknown as there was a misunderstanding with PMS when the probe was returned with the outcome that the FSSP was modified for another project before the cause of the failure could be ascertained.

d. Studies of the 2D-C probe response

Our studies of the 2D-C probe undertaken during the 1979 field season indicate that the instrument undercounts particles in the smaller size channels (midpoints 25 - 175 μm). This is most likely due to the reduced depth of field (DOF) in those channels; however, the DOF corrections supplied by PMS overcorrect the concentrations in these channels.

The 2D-C probe was operated in the wind tunnel at the Elk Mountain Observatory while the mountain was enveloped in a cap cloud. Occasionally during its operation (or when the 1D-C probe was operated) oil coated glass slides were exposed in the wind tunnel near the probe, yet not interfering with the airflow. Ice particles were collected on these slides which were photographed in a bath of cold hexane. These photographs were later used to count and size (in 20 μm bins) the ice particles. Many of the oil-hexane (O-H) slides were overexposed; the crystals which were collected tend to clump together and make counting difficult.

Only one O-H slide, exposed on 3 March 1979, was suitable for a comparison with data taken simultaneously with the 2D-C probe. For a 1 min average, centered around the O-H exposure time, the counts per channel from the 2D-C probe were compared with those from the O-H slide (the 20 μm bins had been mapped into 25 μm bins) to determine a "counting efficiency". This value is plotted against particle size in Figure 15. Also shown are the counting efficiencies found from PMS' DOF values. For

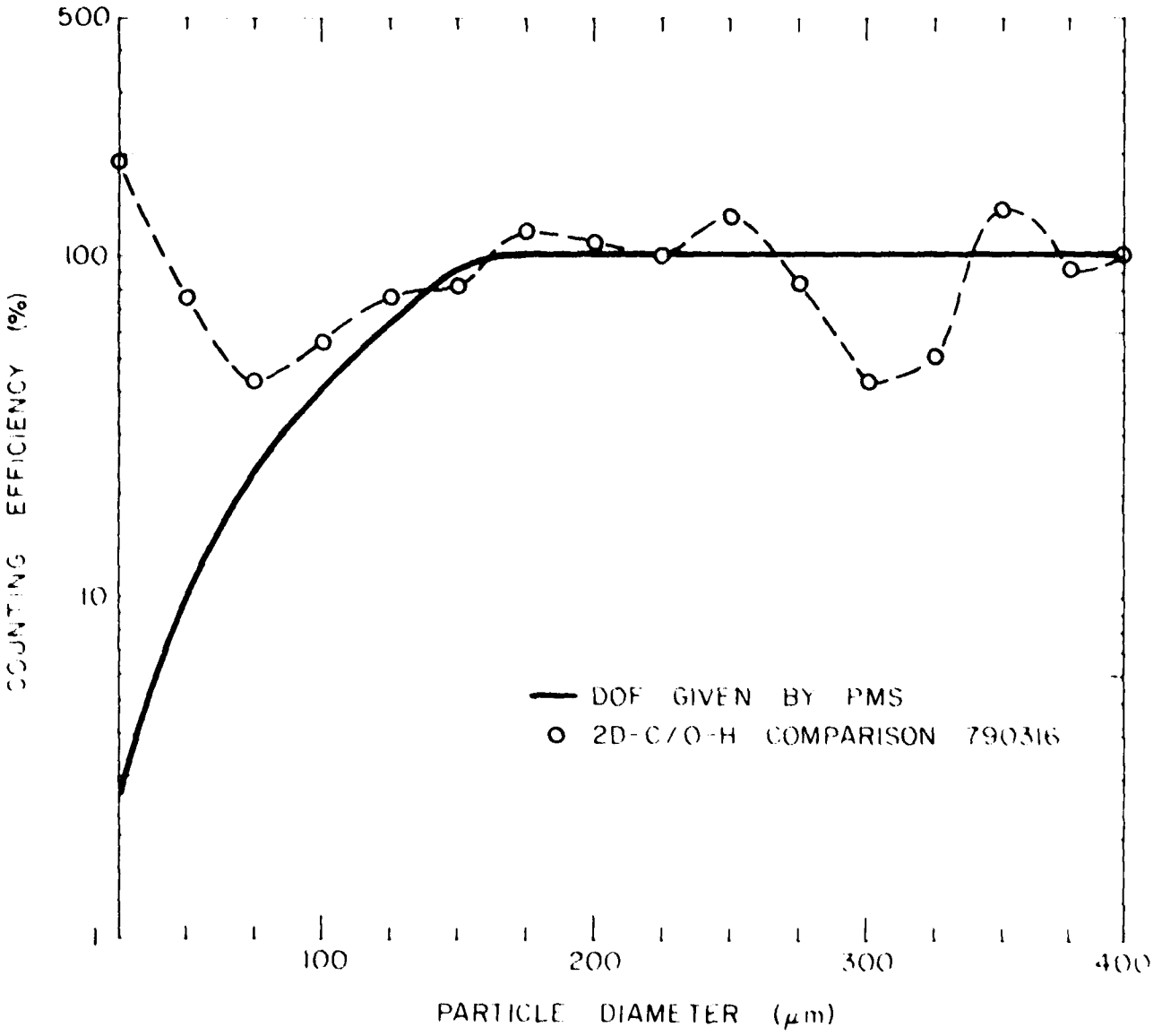

Figure 15 Counting efficiency plotted against particle diameter for a comparison between 2D-C and 0-H data collected at the Elk Mountain Observatory 16 March 1979 at 1321 MST. The 0-H slide was exposed for 2 s; the 2D-C data is a 1 min average centered on the 0-H exposure time. The method for deriving counting efficiency is explained in the text. The solid line represents the counting efficiency predicted by PMS.

most channels the probe response closely resemble, that predicted by PMS. The first channel (mean diameter 25 μm) appears to be subject to a lesser loss of DOF than predicted. More 0-H slide comparisons will be necessary to determine if this overcounting tendency is unique to this sample or a consistent feature (for this reason we have not calculated "effective DOF's for the 2D-C as we have done for the 1D-C). This analysis assumes that the probe will either detect or miss entirely particles, depending on the position of the particle within the beam; possible mis-sizing of out-of-focus particles is thus not considered.

Our comparisons of 2D-C data with 0-H slides in the past have indicated that the use of PMS' small channel corrections result in excessively high ice particle counts in these channels, which leads to extremely high total concentrations and erroneously small mean diameters. We have been analyzing 2D-C probe data using a constant DOF (61 mm), which yields satisfactory mean diameters and concentrations.

The origin of the undercounting problem was further investigated through the use of a movable aperture. This device could be affixed to the 2D-C or 1D-C probe tips and provided a 1 cm wide aperture through which particles could pass. This opening could be moved along the beam length between the probe tips so that the probe response to particles at different positions along the laser beam could be examined.

This aperture was used to investigate how differences in probe response along the beam length contributed to the overall response. Several experiments were conducted in which glass beads of known size ranges were passed through the aperture. Beads of 25-35 μm diameter were not detected by the instrument at all, even at the focal plane of the detector lens. In part this is due to the fact that the clocking rate for these tests was low (to match the low particle velocities); at higher velocities at least a blank frame is expected for these particle sizes. Other bead sizes used were 100-110 μm (peak diameter 100 μm with ~50% of the beads within the 90-110 μm bin), and 250-300 μm (peak diameter 260 μm with ~68% of the beads in the 230-290 μm bins). Some beads were captured on glass slides, then photographed and sized in the same manner as the 0-H slides. A vacuum cleaner was attached to one end of the movable aperture in order to "suck" the beads through.

As beads were sampled further away from the center point of the laser

beam, the bead images (see Figures 16 & 17) were slightly larger and had "donut holes" in their centers. These holes were rare when beads were sampled near the center point of the beam. It could not be determined from these tests whether or not the probe undercounted beads in the smaller size channels as the aperture moved away from the center point. For the 100-110 μm beads there was apparently some noise in the smaller channels which did not change with different aperture positions, and for the 250-300 μm beads few particles were seen in those channels for any aperture position. However, the peak channels did shift to larger sizes as the aperture moved away from the center point (Figure 18). This effect was more pronounced for the smaller size range of beads. Still, for most aperture positions the 20-C image sizes were in reasonable agreement with the mean diameter measured from the O-H slides.

Aperture studies conducted in the wind tunnel were more conclusive. In these studies, the 20-C probe was mounted in the wind tunnel and the movable aperture attached; it was manually moved to the different positions at intervals of several minutes. Counting efficiences were determined by comparing concentrations per channel for aperture positions away from the center point to those measured at the center point. The large ends of the size distributions (sizes $\leq$ 200 μm) were matched graphically to adjust for any differences in total particle concentrations. Since the total time durations of testing were short (less than about 20 min) the size distributions were reasonably constant.

The results of the study are plotted in Figure 19. Channels 2-4 (mean size 50-100 μm) show the greatest DOF effect. Counting efficiencies for these channels decrease significantly as the aperture distance from the center point increases. For example, for the second channel (mean diameter 50 μm) the counting efficiency at 1 cm from the laser end was 47%, while next to the laser end it was 12%, these values for 1 cm from the detector end were 23-37% and near the detector end were 17-29%. The effect on the first channel (mean size 25 μm) is not as great; counting efficiencies were ~10% higher than those of the second channel (ranging from 7-33% and increasing further from the center point).

The response of the 20-C probe at sizes > 100 μm is close to the PMS specifications. The counting efficiencies for the first two channels (midpoints 25 and 50 μm) are somewhat higher than those given by PMS. At

Figure 16 2D-C images of 100-110 μm glass beads recorded on 2 April 1979 at the Elk Mountain Observatory. Elongation of images is due to timing differences with the 2D-C DAS clock. Mobile aperture positions are (a) ∿ 2 cm toward laser side from center point of probe aperture, (b) ∿ 1.4 cm toward laser side and (c) ∿ 0.8 cm toward laser (d) at center point (e) ∿ 0.8 cm toward detector and (f) ∿ 1.4 cm toward detector

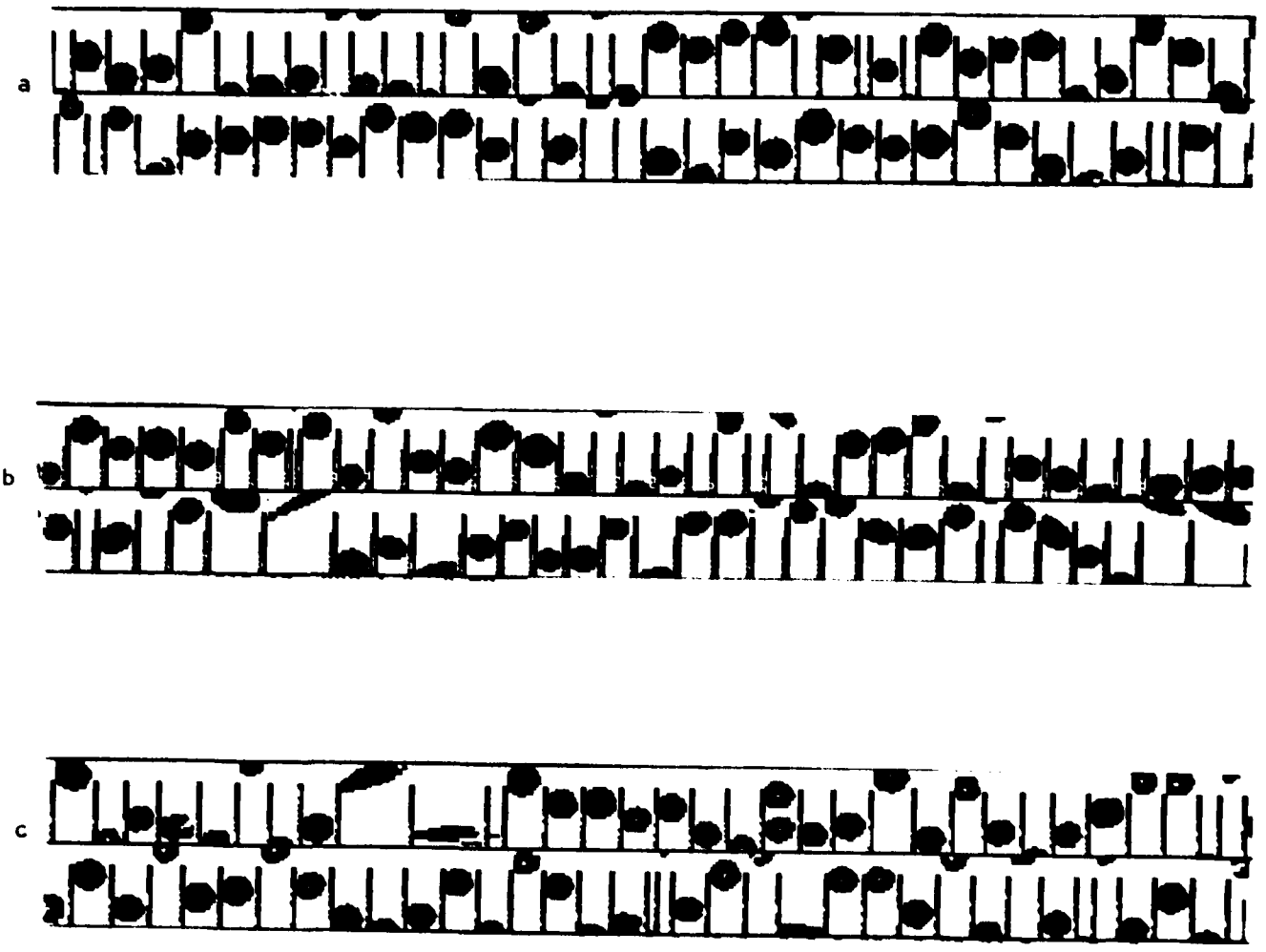

Figure 17 2D-C images of 250-300 μm glass beads recorded on 2 April 1979 at the Elk Mountain Observatory. Elongation of images is due to timing differences with the 2D-C DAS clock. Mobile aperture positions are (a) ∿ 2 cm toward laser side from center point of probe aperture (b) at center point and (c) ∿ 2 cm toward detector.

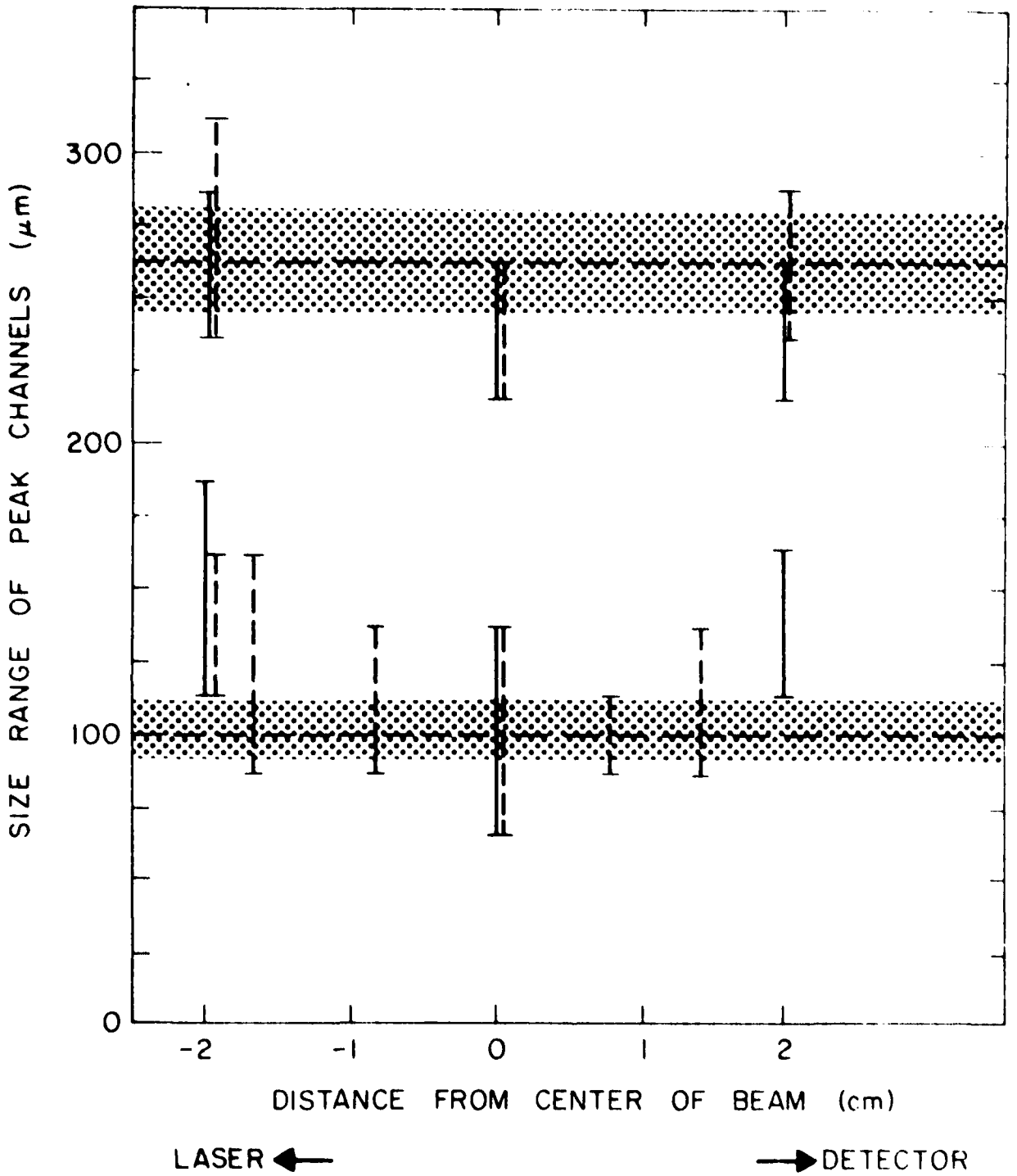

Figure 18 Peak particle size measured by the 2D-C probe plotted against distance from center point of probe aperture. The solid and dashed line intervals represent different sets of samples. The peak sizes for the two sets of beads were 100 μm and 260 μm, shown by horizontal dashed lines, with ~ 50% of the samples within the shaded regions. Data was collected on 4 April 1979 at the Elk Mountain Observatory.

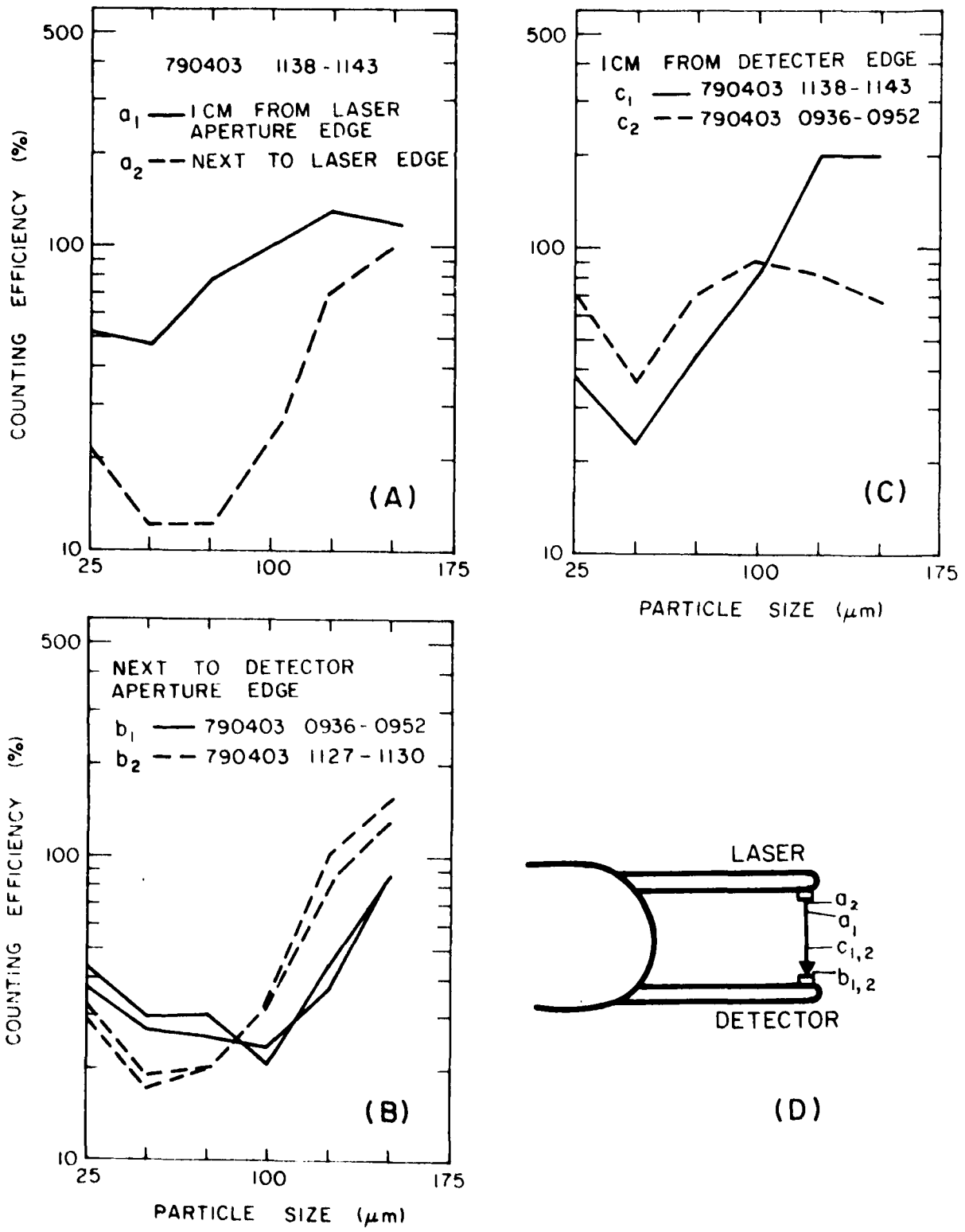

Figure 19 2D-C counting efficiency plotted against diameter for wind tunnel tests using the movable aperture. (a) movable aperture at laser edge and 1 cm from laser edge of probe aperture, (b) aperture at detector edge, (c) aperture 1 cm from detector edge, and (d) schematic of movable aperture positions. Data was collected during the dates and times specified.

this point this cannot be satisfactorily explained; it could be due to mis-sizing of larger particles, light refraction or other noise.

With more O-H comparisons, "effective" depths of field could be determined for the 2D-C probe. These would be used in data analysis to find the true ice particle spectrum from the measured spectrum. At present we will continue to use constant depth of field of 61 mm (limited by the probe aperture).

The 2D-C probe data shows counts in the smaller channels (sizes < 100 μm) for both the bead sizes (100-110 μm and 250-300 μm beads), but there is up to now no real proof that these are real and not noise or mis-sized counts. The probe did not detect 25-35 μm beads at any point along the laser beam for the speeds used; while 100-110 μm beads were detected along the entire beam length. Unfortunately beads in the range between 35-100 μm diameters were not available during testing. Whether the probe detects small (< 10 μm) ice particles, and with what efficiencies, is a crucial problem, and we intend to focus much of our 1980 field work to finding an answer to this.

e. Studies of the 1D-C probe response

The results of our investigations of the 1D-C probe are in many ways similar to those obtained from the 2D-C probe studies. The probe undercounts particles in the smaller channels, due to decreased DOF's for these sizes ($\lesssim$ 140 μm). There also appears to be an undercounting problem in the larger channels ($\gtrsim$ 240 μm).

Eleven O-H slides were available for comparison with 1D-C data. As for the 2D-C - O-H comparison, the 1D-C data was a 1 min average around the time of the O-H slide exposure time (usually 2-10 s). Counts per channel were compared in order to determine counting efficiencies. The results are plotted in Figure 20. PMS includes a "sample probability" for the first three channels. This is a theoretical value, ranging from 26% for the first channel to 89% for the third and describes the probability that a particle in that size range is correctly detected. The predicted counting efficiencies with and without this factor are also plotted in Figure 20. The general shape of the data curve agrees well with the PMS values, but it does appear that the counting efficiencies are higher in the low channels than those given by PMS. The data seem to match most closely the curve obtained by excluding the sampling probability. In

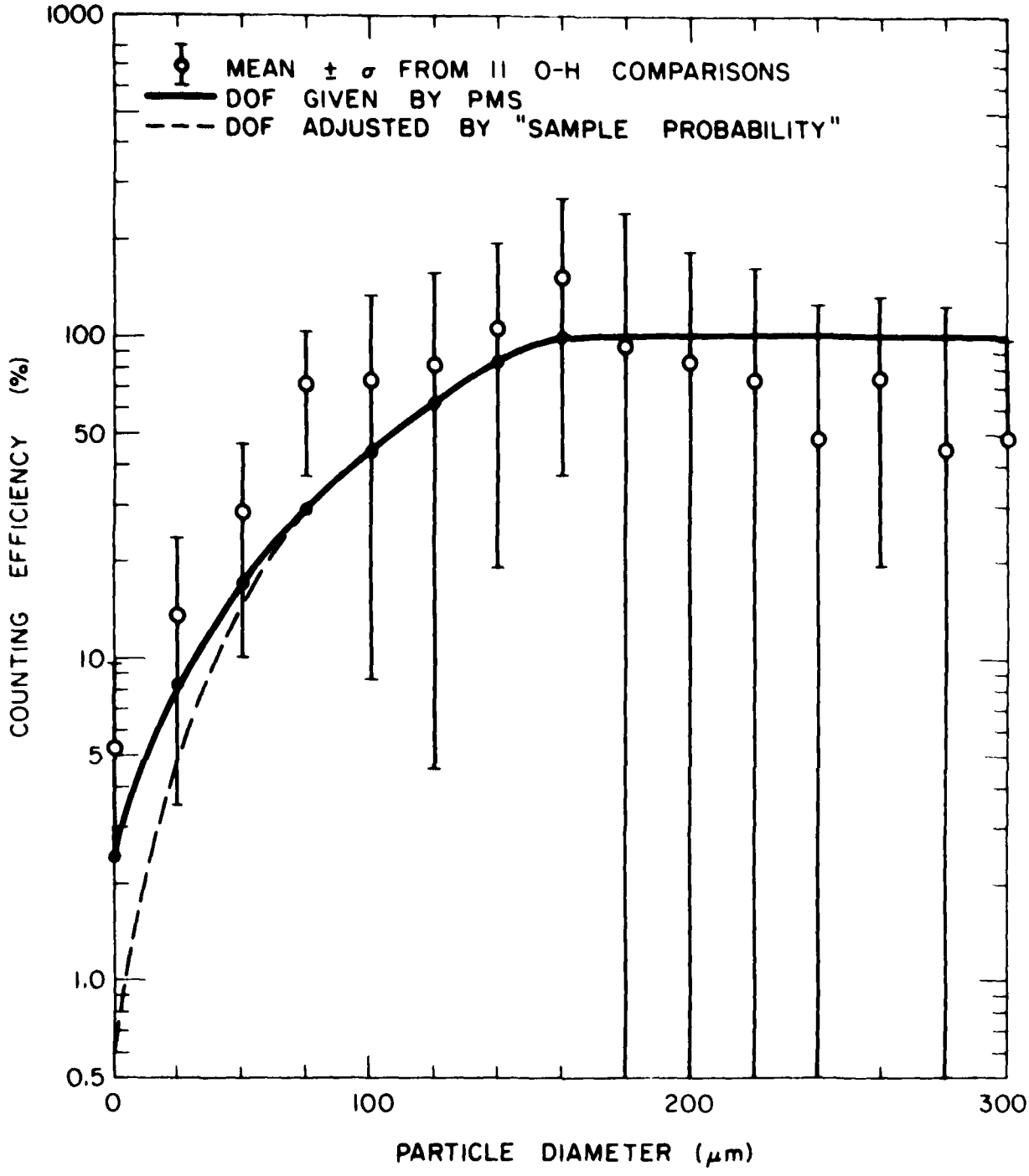

Figure 20 Counting efficiency plotted against ice particle diameter for 1D-C data (o) and those predicted by PMS' depth of field values (——— and -----). 1D-C data is based on 11 O-H slide comparisons; means and standard deviations are shown. The data were collected on 16, 17 and 25 March at the Elk Mountain Observatory.

addition, the higher channels (sizes > 240 μm) undercount particles. The reason for this undercounting is not understood.

In determining the mean size of the sampled beads, and of ice particles sampled in the wind tunnel, the DOF's supplied by PMS were used without inclusion of the sample probabilities, even though the O-H comparison data suggest that these values may be slightly small. However, as shown in Figures 21 and 22, they yield the best agreement between mean diameters and their dispersions as determined from the O-H slides. Using a constant DOF gives mean diameters too large and dispersion coefficients too small; including the sample probabilities in the DOF's give diameters too small and dispersions too large. The shapes of the spectra obtained from using the PMS DOF's match most closely those from the O-H data (see Figure 23).

In a manner similar to that used from the 2D-C probe, the response of the 1D-C probe was examined using the mobile aperture and glass beads. The same size ranges of beads were used as in the 2D-C tests, except when the beads were sized by hand only those beads with diameters less than 310 μm were included. (The 25-35 μm beads were not available for these tests.

The mean diameters of the sampled beads as measured by the 1D-C probe are plotted against distance from the center point of the laser beam in Figure 24. There is a notable increase in measured mean diameter as the aperture moves away from the center point, and, as for the 2D-C, this is more pronounced for the smaller glass beads. The 1D-C probe response to the larger beads is nearly constant for all aperture positions, except for the undersizing that seems to be occurring at the center point of the beam. The 1D-C mean diameters are in good agreement with those measured for the beads for most aperture positions.

Counting efficiencies for each channel were also determined for the bead tests. Counts per channel for aperture positions away from the center point were "normalized" to those measured at the center point by comparing the total concentration of counts for sizes 180 μm and larger (these channels did not appear to be affected by changes in aperture position), and adjusting the remainder of the spectrum accordingly. The counting efficiencies for the smaller channels were then derived. Figure 25 shows the results of these calculations. Channels 2-4 (mean size

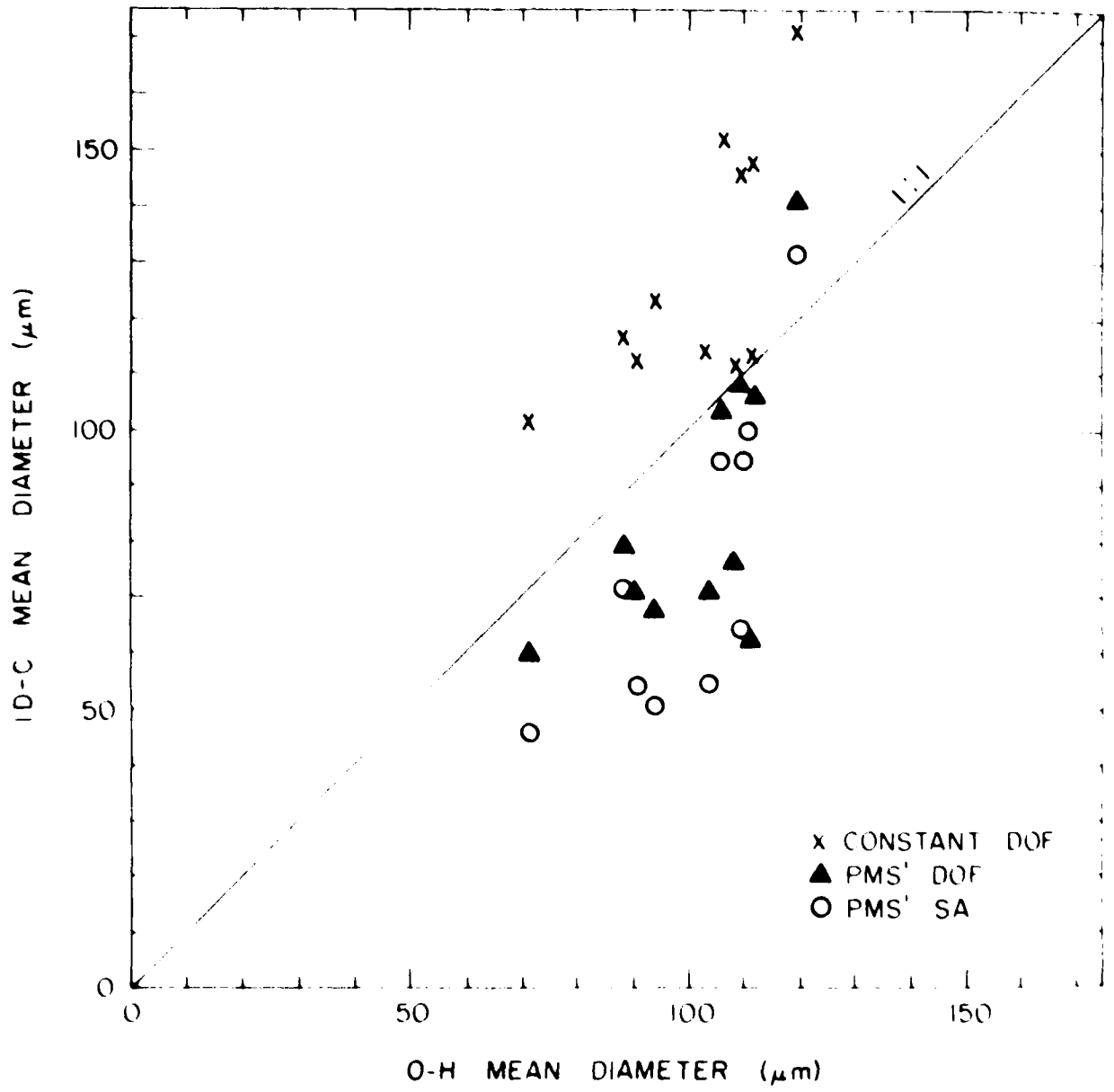

Figure 21 1D-C mean diameter plotted against 0-H mean diameter for 10 samples collected at the Elk Mountain Observatory. A constant DOF (X), PMS' DOF (▲) and PMS' SA (sample area, which includes "sample probability") (O) were used in data analysis.

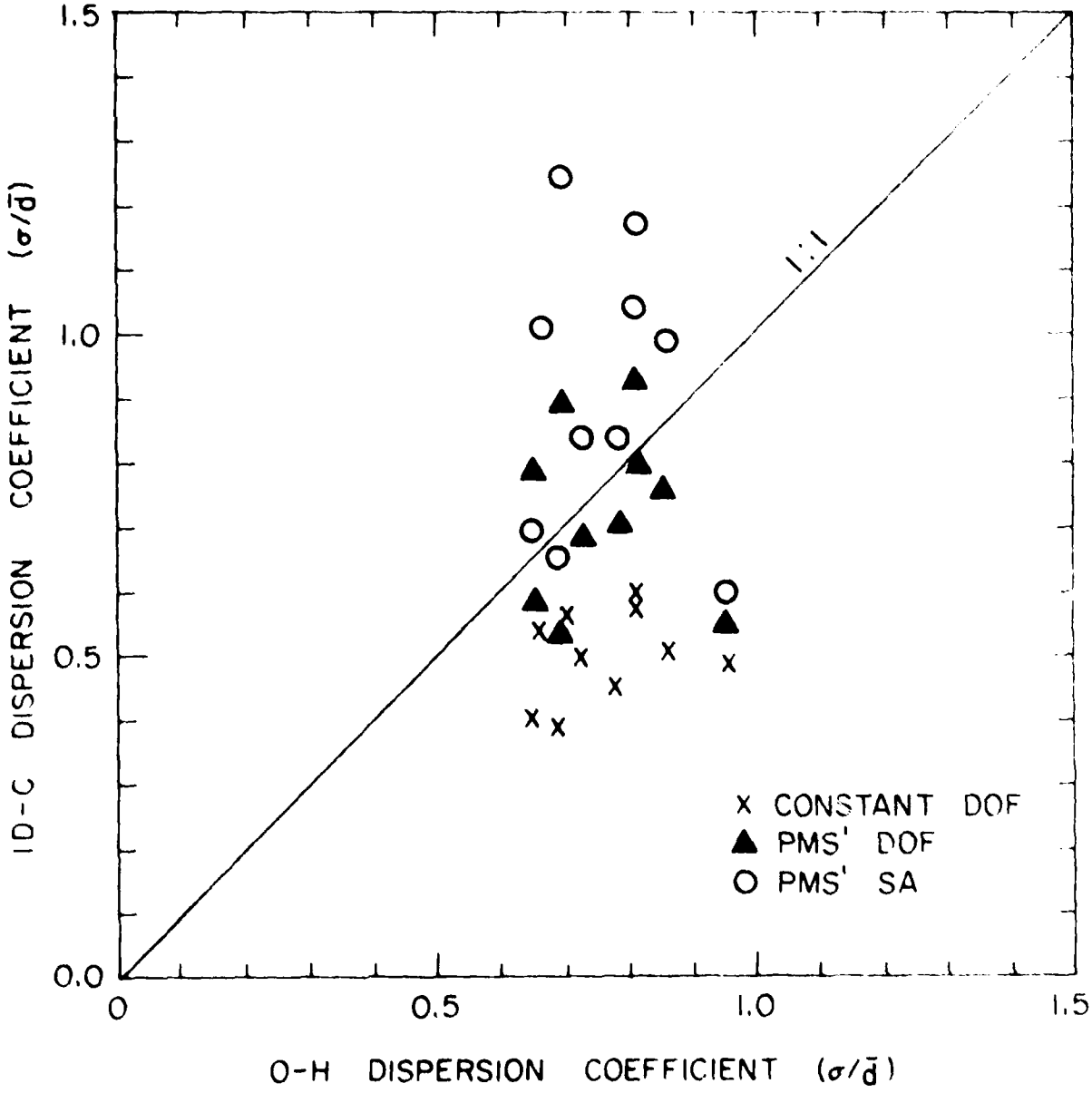

Figure 22 1D-C dispersion coefficients ($\sigma/\bar{d}$) plotted against 0-H dispersion coefficients. Samples are the same as shown in Figure 21.

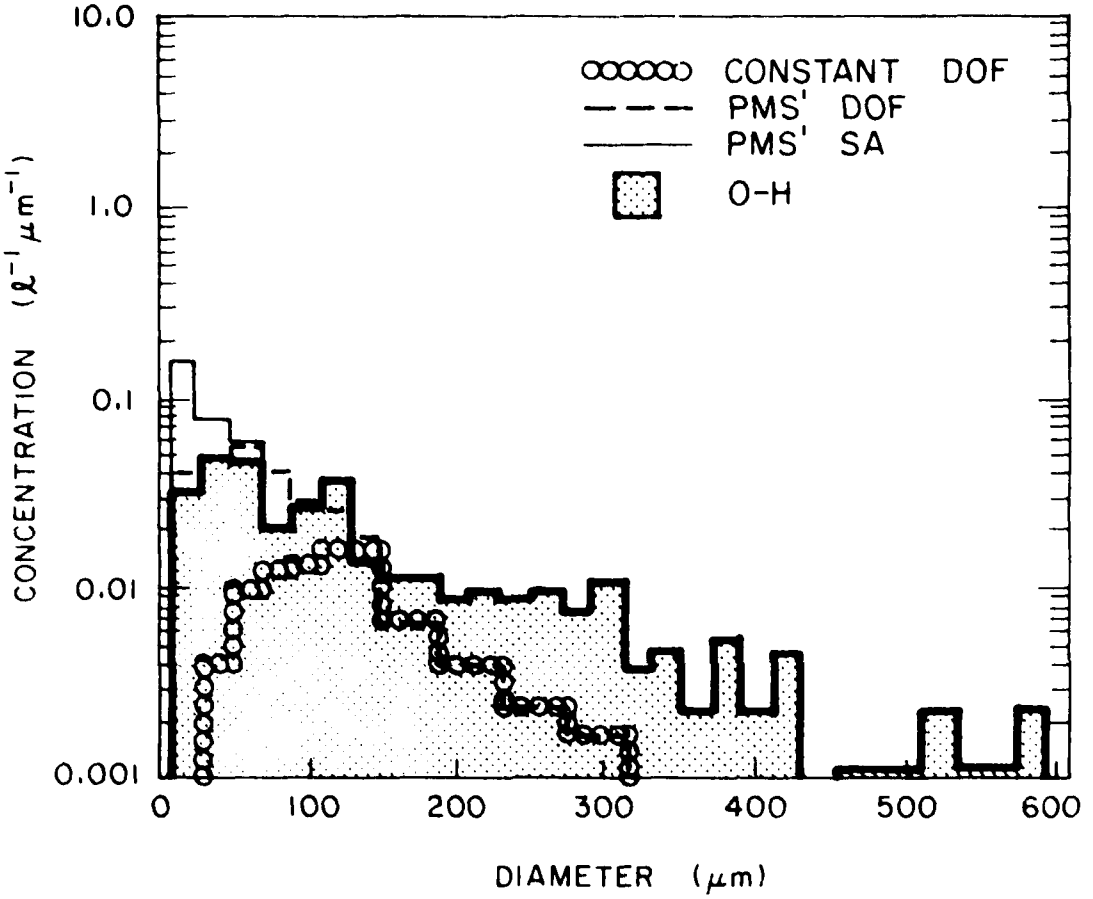

Figure 23 Concentration plotted against ice particle diameter for O-H and 1D-C data taken at Elk Mountain Observatory at 0033 MST 17 Mar 1979. O-H slide was exposed for 10 s, the 1D-C data is a 1 min average taken around the O-H exposure time. The different 1D-C DOF's used are shown in the diagram.

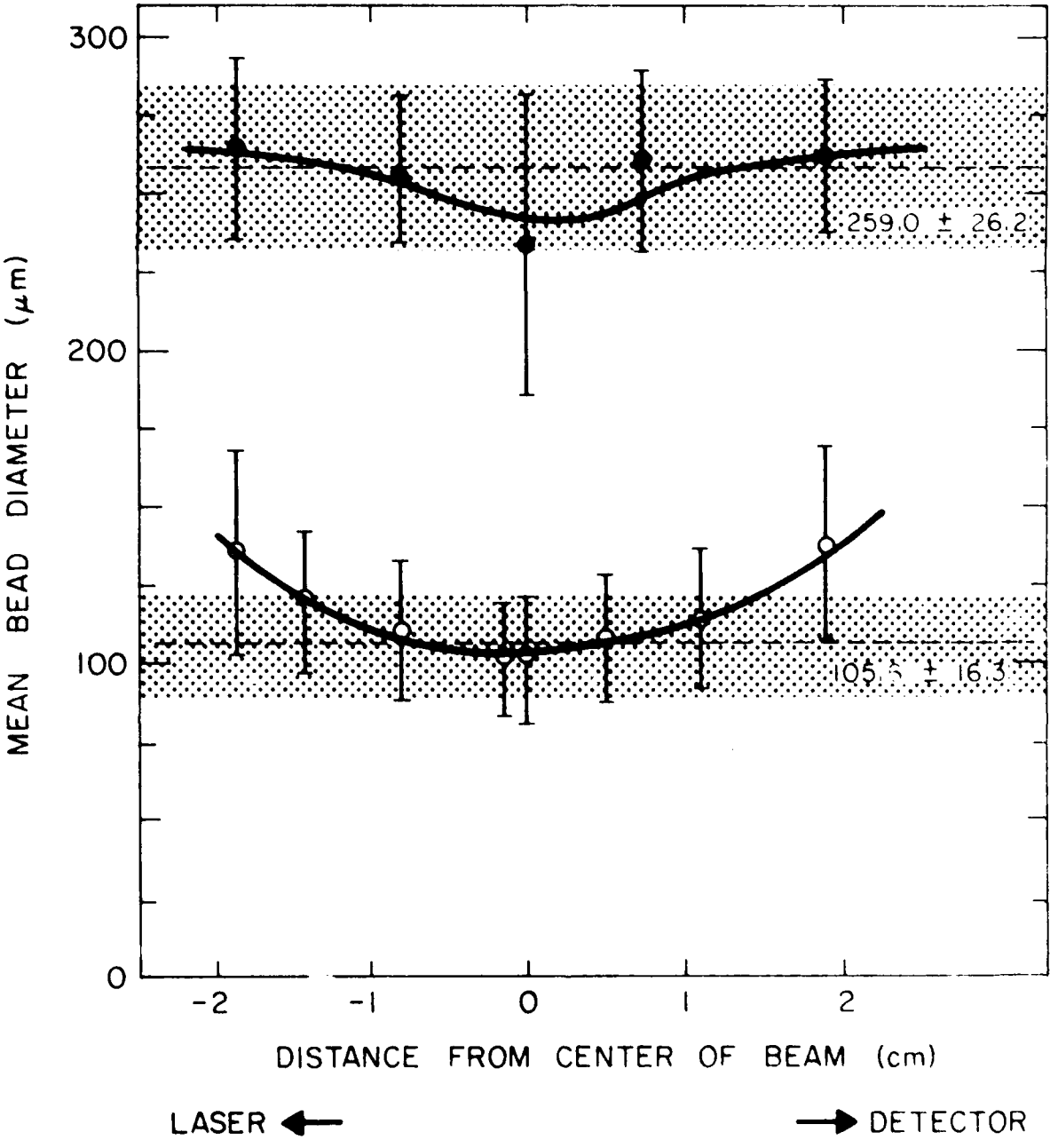

Figure 24 Mean bead diameter(±standard deviation) plotted against distance from the center point, from the glass bead tests using the movable aperture. Data collected at the Elk Mountain Observatory on 4 April 1979. True mean diameters and their standard deviations are shown by shading, the solid line represents the trend of the data.

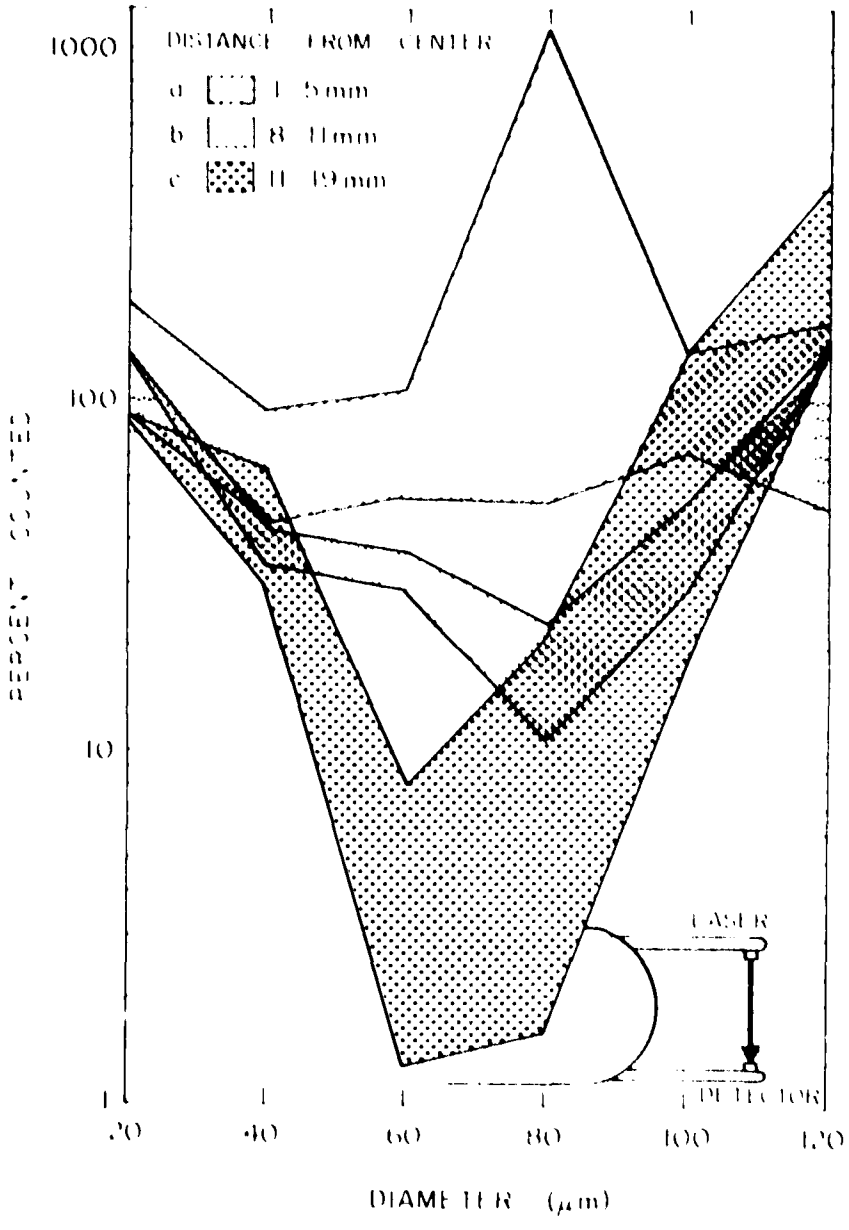

Figure 25 Percent of beads counted plotted against diameter for the data set shown in Figure 24. Data are grouped for ranges of aperture positions; distances from center of movable aperture to mid point of probe aperture were 1-5, 8-11, 11-19 mm.

40-80 μm) are those most affected by changes in the aperture position. Counting efficiencies for the first channel (mean size 20 μm) remain fairly high (90-190%) for all positions. The counting efficiencies for the second through fourth channel are those most affected by changes in the aperture position; for example, the counting efficiencies for the third channel (mean size 60 μm) range from 52-106% when the aperture is 1-5 mm from the center point, to 1.3 - 7.9% when the aperture is 11-19 mm from the center point.

Aperture tests were also conducted in the wind tunnel, where ice crystals and blowing snow particles were sampled. The 1D-C probe was operated with the movable aperture, and the 2D-C was run alongside to monitor the size distributions of ice particles in the cloud. These tests were performed on several days (see Table 1). Counts per channel were recorded for the different aperture positions, and compared to those recorded for the aperture at the center point. The concentrations per channel were adjusted for changes in the total cloud ice particle concentration (as measured by the 2D-C probe) before counting efficiencies were determined; the shape of the size distribution did remain nearly constant.

The counting efficiencies obtained from the wind tunnel tests were higher than those from the glass bead tests yet they display the same tendencies (see Figure 26). As the aperture moves from the center point of the probe aperture the counting efficiency of channels 2-5 decreased significantly, while that of the first channel remains fairly high. The counting efficiencies from the glass bead tests were fairly symmetric about the center point of the laser beam. For these wind tunnel tests some degree of asymmetry about the center point is observed; the actual optical center point may be displaced slightly toward the laser side of the probe aperture. Recall that the overall effect (as shown in Figure 15) observed was that the probe undercounted in higher channels. This is the case for the aperture position about 2 cm from the center point on either side, however, at the extreme edges the probe overcounts. If this overcounting occurs only at the extreme ends of the laser beam, for a small fraction of its entire length, these results are not necessarily inconsistent with the overall results. The average taken over the entire beam length could still result in undercounting.

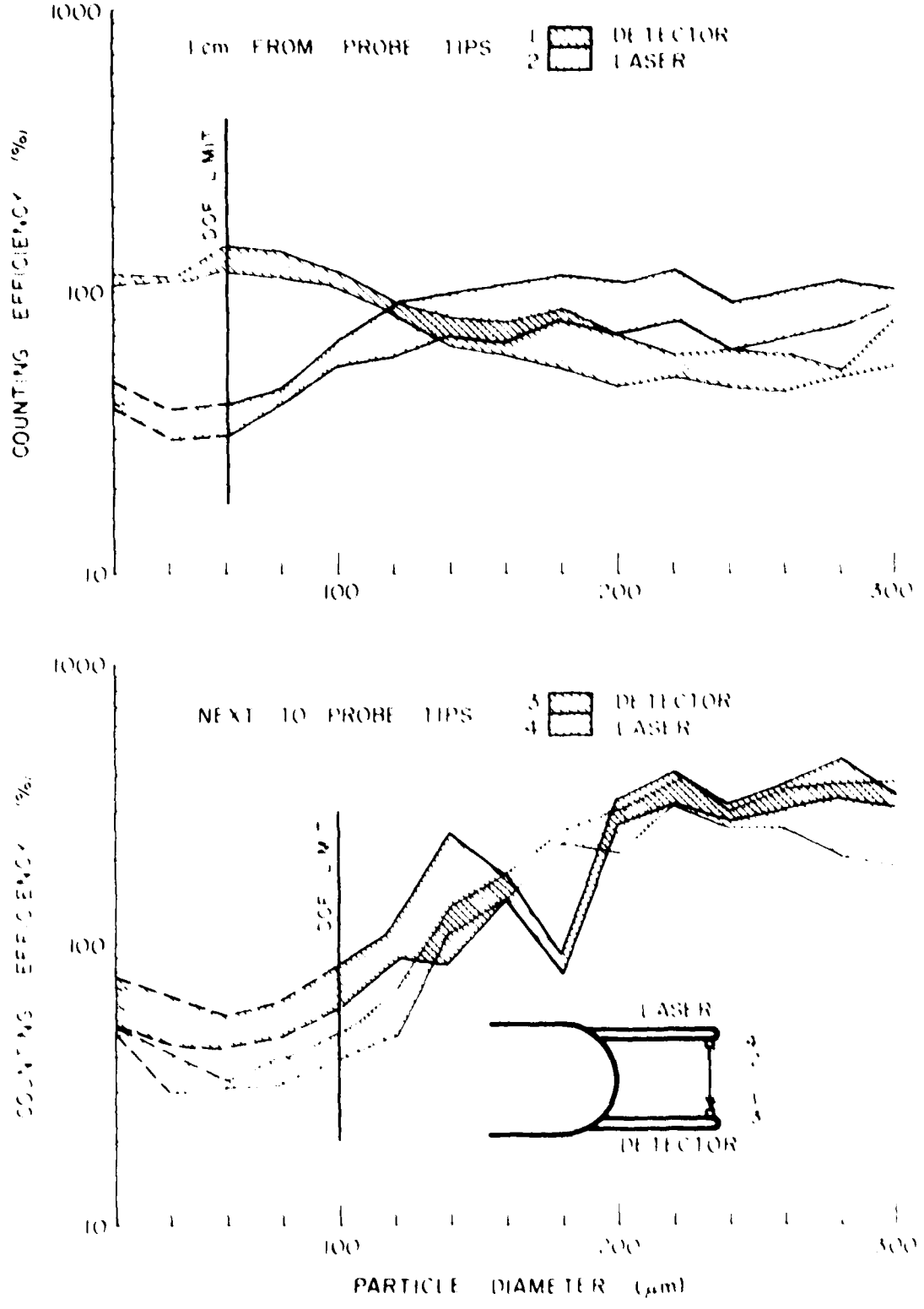

Figure 26 Counting efficiency plotted against diameter for tests using the movable aperture in the wind tunnel at the Elk Mountain Observatory. Aperture positions are as shown. The range of several 30 s averages of ID-C are indicated. The depth of field limits are shown by a vertical line. Data was collected on 2 April 1979.

The total ice particle concentrations measured by the 1D-C probe are about 25% lower than those measured simultaneously by the 2D-C probe (for particle size $\leq$ 300 μm only). The undercounting observed in the higher channels of the 1D-C probe may account for this. In the lower channels where the undercounting is due to particles being out of the depth of field, the PMS corrections for small particle sizes which were used actually overcorrect slightly for concentration.

Knollenberg (1975) has determined a set of relations between measured versus actual crystal size for various ice crystal types sampled by the 1D-C probe. The correction of II ice (large and small irregular snow) has been applied to the 1D-C data set for comparison with 0-H and 2D-C data. The results are closer agreement in mean diameters (see Figure 27) and in the shape of the particle spectra (see Figures 28 and 29). These corrections particularly improve the larger end of the spectrum, where it appears that the 1D-C probe is undercounting.

The depth of fields for the 1D-C probe are listed in Table 2. This table includes PMS' depth of fields- with and without the "sampling probability"-and those calculated from the counting efficiencies found from 1D-C - 0-H data comparison. Those DOF's found for lower channels ($\leq$ 180 μm) are smaller than the PMS values, however, those for larger channels ($\geq$ 240 μm) are generally larger. It is our intention to verify the consistency of these values during the 1980 field season.

The undercounting of particles in small size ranges ($\leq$ 100 μm) for the 1D-C probe can be explained as being due to the reduced DOF's in these lower channels. The quoted DOF's actually slightly overcorrect for concentrations in these channels.

As for the 2D-C probe, however, we cannot be sure that these counts are real. During the glass bead tests on the 1D-C probe using the movable aperture reductions in particle counts in the small channels were not noted as the aperture was moved from the center point of the beam. This was not observed in the 2D-C probe data; counts in the first three channels remained nearly constant at all aperture positions. The reduction in counts is expected if the DOF's were indeed smaller for those channels. This supports the

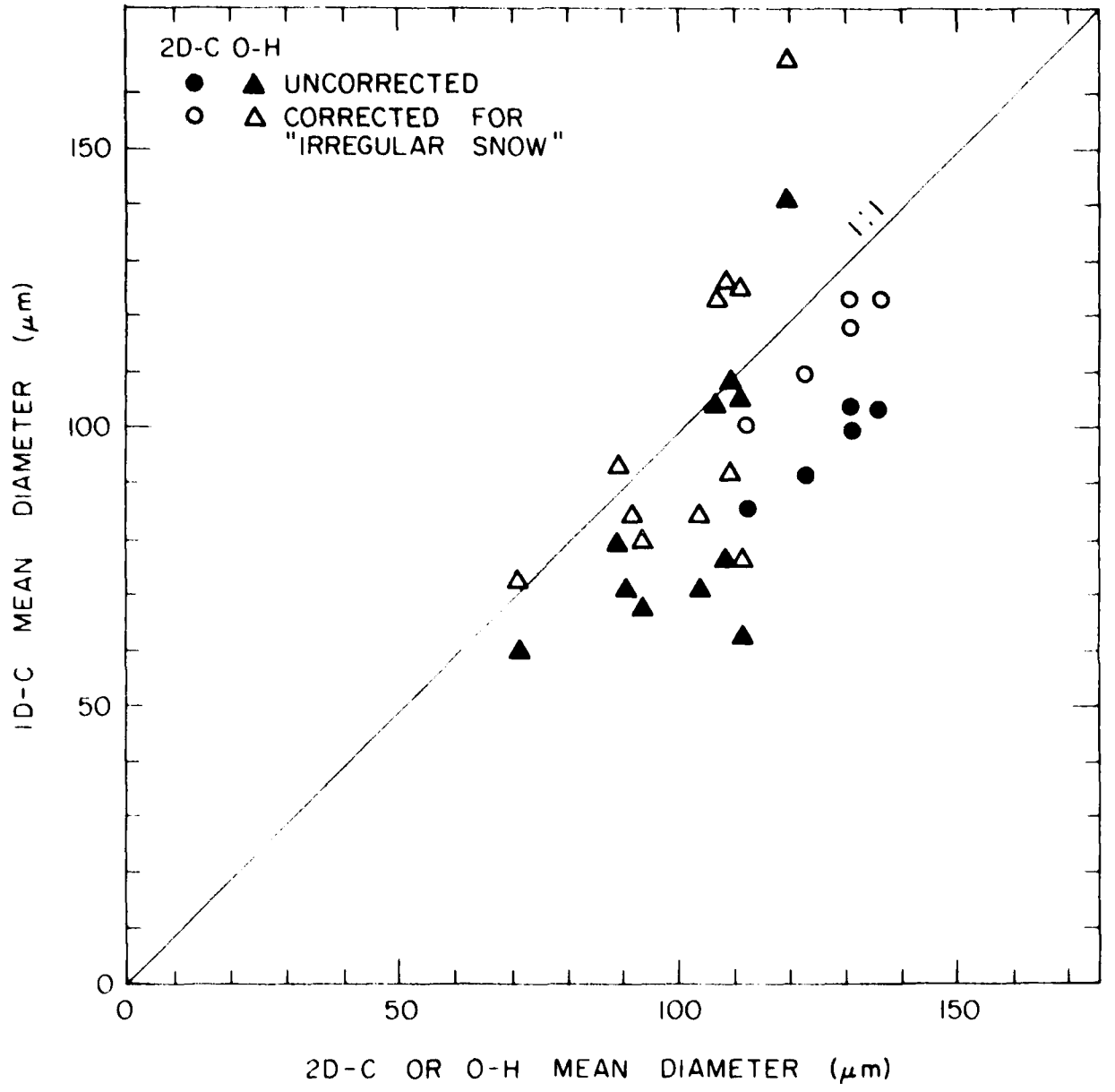

Figure 27 1D-C mean diameter plotted against O-H (triangles) or 2D-C (circles) mean diameter. Data for uncorrected closed symbols) and corrected (Knollenberg, 1975) as "irregular snow" (open symbols) are indicated. O-H data were 2-10 s exposures; 1D-C comparisons are 1 min averages taken around the O-H exposure times; 1D-C - 2D-C comparisons are 30 s averages.

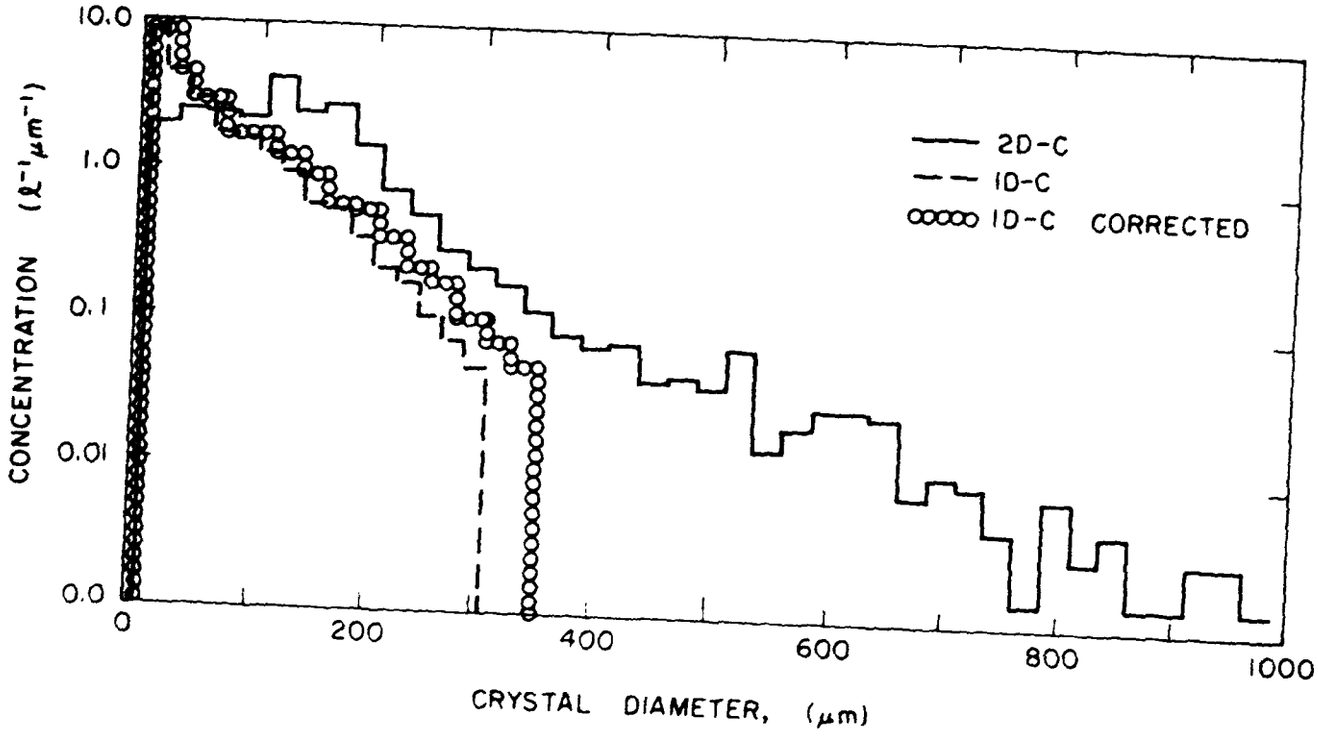

Figure 28 Concentration plotted against diameter for 1D-C -2D-C probe comparison from 3 April 1979 at the Elk Mountain Observatory. 1D-C data uncorrected (-----) and corrected (ooooo) as "irregular snow" (Knollenberg, 1975) and corresponding 2D-C data (———) are shown.

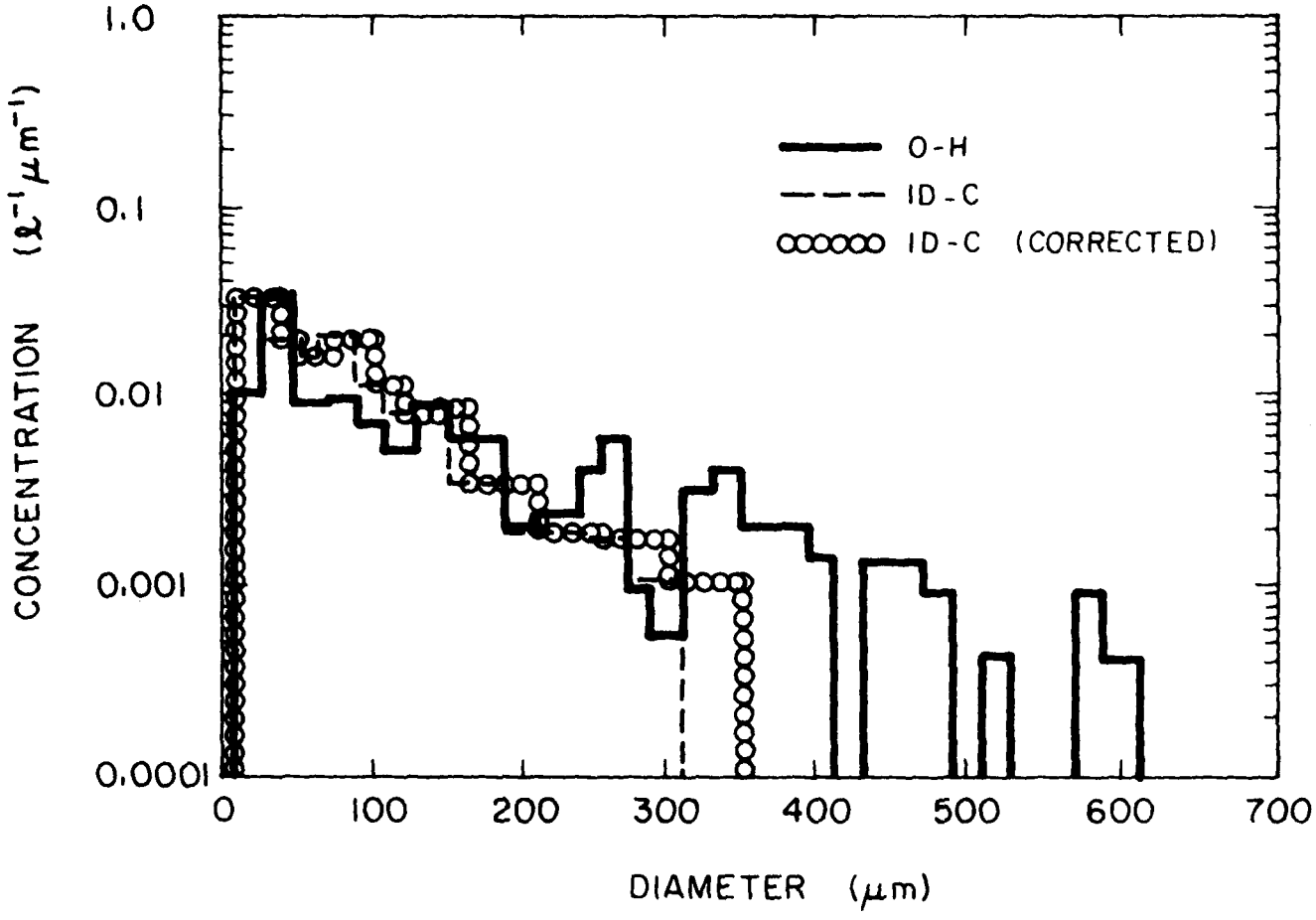

Figure 29 Concentration plotted against ice particle diameter for data collected at the Elk Mountain Observatory at 1020 MST on 17 March 1979. ID-C data uncorrected (-----) and corrected (ooooo)as"irregular snow" (Knollenberg, 1975) and corresponding O-H (———) data are shown. The O-H slide was exposed for 10 s; the ID-C data are a 1 min average taken around the O-H exposure time.

TABLE 2 Depth of Field vs. Diameter
PMS 1D-C Probe Model OAP-200X

CHANNEL	MEAN DIAMETER (μm)	DEPTH OF FIELD (mm)		
		FROM DATA	PMS *1	PMS *2
1	20	3.23	1.45	0.38
2	40	8.36	4.82	2.99
3	60	17.39	10.14	9.02
4	80	43.31	17.03	Same as
5	100	44.53	26.68	PMS *1
6	120	49.41	32.82	
7	140	64.66	50.84	
8	160	92.72	61.00	
9	180	57.95	"	
10	200	51.24	"	
11	220	44.53	"	
12	240	29.89	"	
13	260	45.75	"	
14	280	27.45	"	
15	300	45.75	61.00	

*Includes "sample" probability

clare that the 1D-C probe does detect small particles but is not conclusive.

The undercounting which is apparent for the larger channels (sizes 240 μm) is disturbing. This can in part be compensated by use of Knollenberg's (1976) correction schemes, which would indicate that part of the undercounting is due to undersizing of ice crystals. The problem, however, appears more serious than can be explained by Knollenberg's calculations or the glass bead tests (recall that at the center point of the beam, the 250-300 μm glass beads were undersized slightly). This problem calls for further attention and shall be examined more thoroughly during the next field season.

t. Study of the response of the ASSP and FSSP to ice particles

Studies were made of the response of the ASSP and FSSP to ice particles by finding portions of data in which no water droplets were found and only ice particles were present. In the case with the ASSP, the absence of cloud droplets was confirmed by sampling the cloud with the cloud gun, and in the case involving the FSSP, the test was run on a cloudless period when the ice particles were formed artificially at the wind tunnel mouth using propane seeding. Figure 30 shows the spectral distribution of the ASSP for four 30 s periods, and Figure 31 shows the response of the FSSP averaged over four 30 s periods. For the case of the ASSP, a representative ice particle distribution as measured by the 2D-C probe is shown in Figure 32, and a representative distribution of ice particles during seeding is shown in Figure 33. Small ice crystals were more numerous for the FSSP tests, but the FSSP data has some noise in the lower channels, so it cannot be ascertained from these data whether the FSSP spectra produced by ice crystals (Figure 31) are generally different, or not, from those measured by the ASSP (Figure 30). Further demonstration of ice-produced spectra in the ASSP have been obtained by comparisons with 1D-C data. Data from the 1D-C probe was used since, as has been shown in a previous section of this report, we are more confident of the response of this probe than we are of the response of the 2D-C probe in the overlap region (sizes up to about 45 μm). On several different field days the 1D-C and ASSP were run together in the wind tunnel. Soot coated cloud gun slides were exposed during these runs, either

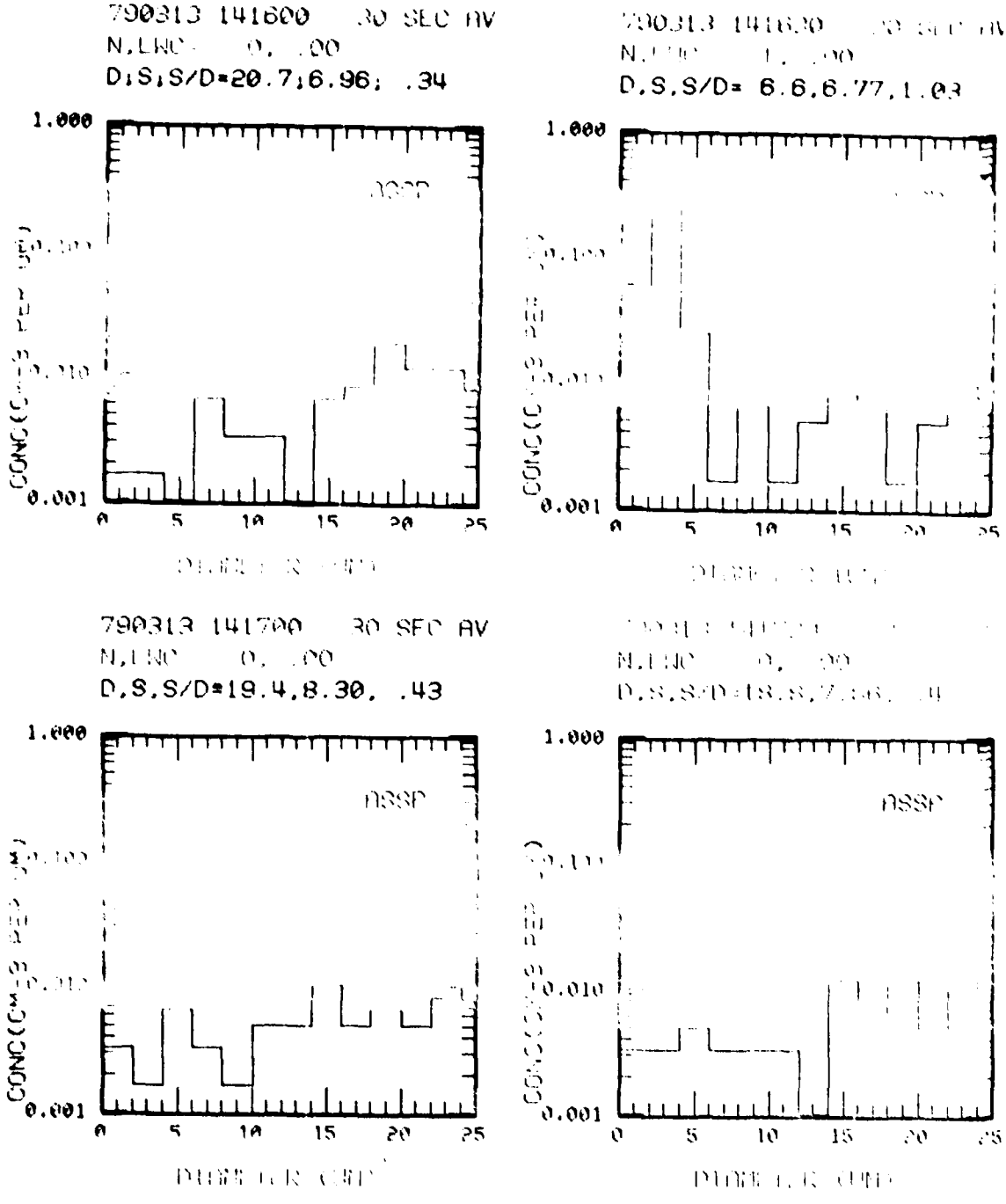

Figure 30 Four examples of the ASSP spectrum (concentration versus diameter) measured when only ice particles (and few or no water droplets) were present. These samples were taken at 1416-1418 MST on 13 March 1979. Droplet concentration in cm^{-3} (N), liquid water content in gm^{-3} (LWC), mean diameter in microns (D), standard deviation in microns (s) and variance (s/D) are given for each 30 s average.

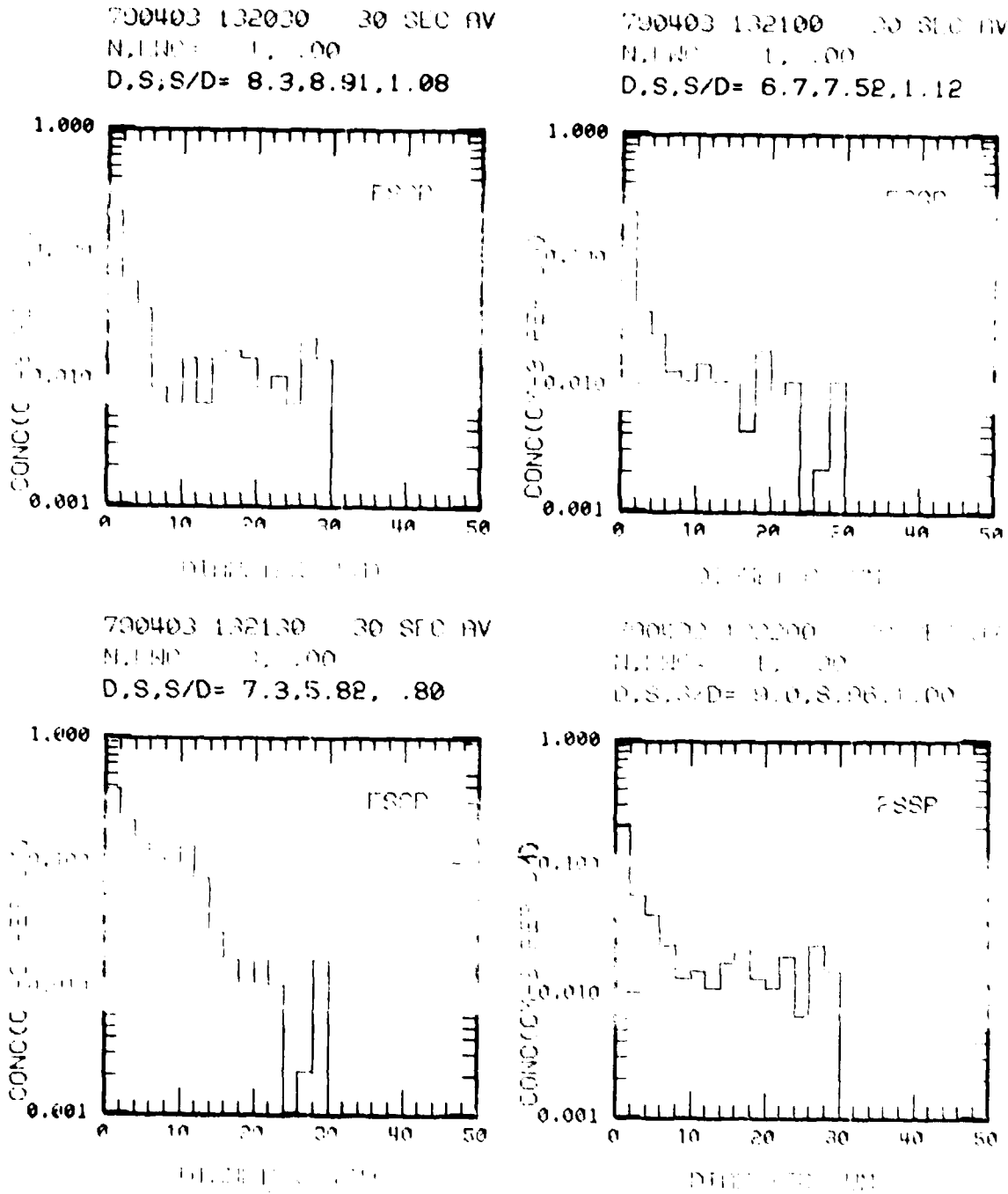

Figure 31 Four examples of the FSSP spectrum measured when only ice particles and few or no water droplets were present. These samples were taken at 132030-132230 MST on 4 April 1979. The key to the values listed above the the graphs is given in the caption for Figure 30.

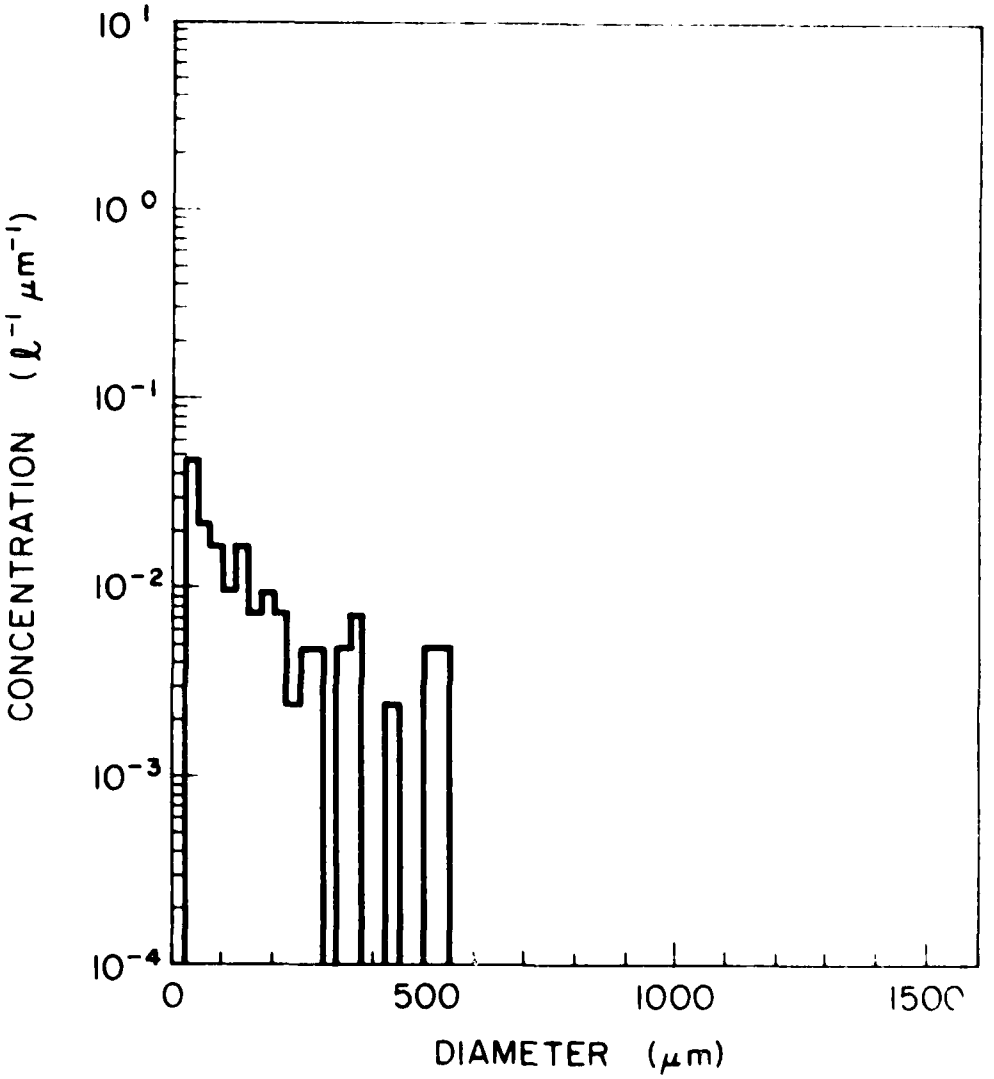

Figure 32 Concentration plotted against diameter for ice particles sampled by the 2D-C probe from 1414600-1416?9 MST on 13 March 1979. This sample corresponds to the ASSP data presented in Figure 30. The ice particle concentration as measured by the 2D-C probe was 4.3 ℓ^{-1}, the mean diameter was 148.1 μm.

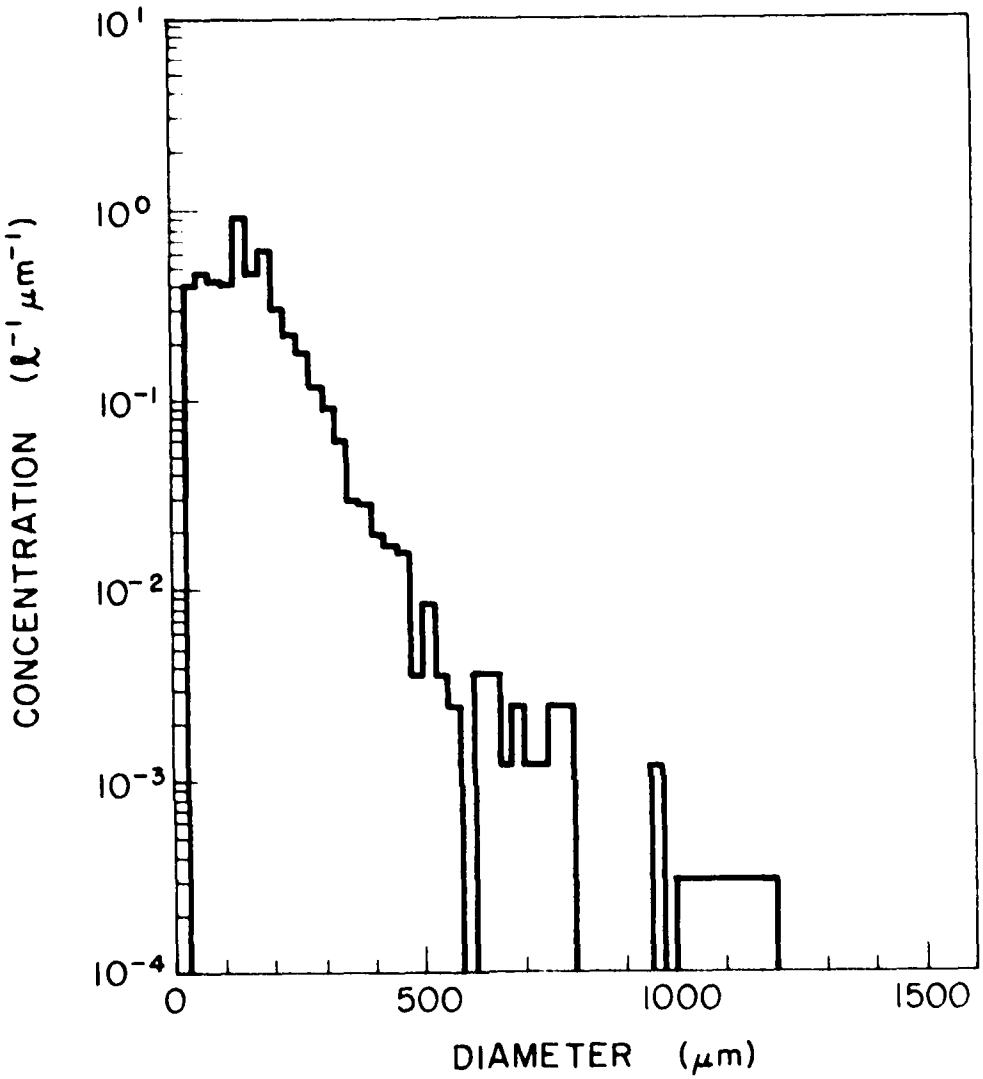

Figure 33 Concentration plotted against diameter for ice particles sampled by the 2D-C probe from 132030-132059 on 4 April 1979. This sample corresponds to the FSSP data presented in Figure 31. The ice particle concentration measured by the 2D-C probe was 121 ℓ^{-1}, the mean diameter was 155.6 μm.

to provide a cross-check of the actual cloud droplet spectra, to insure that no droplets were present in an ice cloud.

Thirty second averages of the data around the cloud gun exposure time were taken for comparison. The 1D-C data was analyzed using the "effective depths of fields" resulting from our studies of the 1D-C probe (see Table 2). This gave our best estimate of the ice particle spectra.

In the presence of ice particles, the ASSP spectra show flat distributions of counts in all channels. When no cloud droplets were present, counts are seen in all channels, and concentrations are quite low (but do not correspond to the true ice particle concentrations). In mixed clouds, the droplet "spike" is superimposed upon this background of counts. Several examples of this are shown in Figures 34-36. The 1D-C, ASSP and cloud gun spectra are graphed on the same scale. The flat distributions in the higher channels are clearly distinguished from the droplet spectra. It is important to note that these flat distributions, presumably resulting from ice particles, are not seen in all-water clouds.

The three spectra shown represent widely varying ice particle concentrations as measured by the 1D-C probe: 1.8, 43, and 190 ℓ^{-1}, a variation of two orders of magnitude. (The corresponding droplet concentrations change by < 200%, they are: 293, 116, and 372 cm^{-3} as measured by the ASSP). The flat "tails" of the ASSP spectra change almost exactly in proportion with the ice particle concentrations. Thus, it appears to be quite clear that the flat distributions in the ASSP data are associated more closely with the concentrations of ice particles than with those of cloud droplets.

Similar observations have been documented for the FSSP, that is, in the presence of ice particles, a flat distribution of particle counts is seen across the whole range of the instrument, with a superimposed droplet "spike".

In the presence of the ice particles, the ASSP and FSSP cloud droplet probes experience counts distributed fairly evenly over the entire sampling range. These counts do not exhibit a one-to-one correspondence with ice particle concentrations as measured by the 1D-C probe; sizes and concentrations are not correctly measured. It may be that each ice particle passing through the ASSP or FSSP laser beam results in several counts.

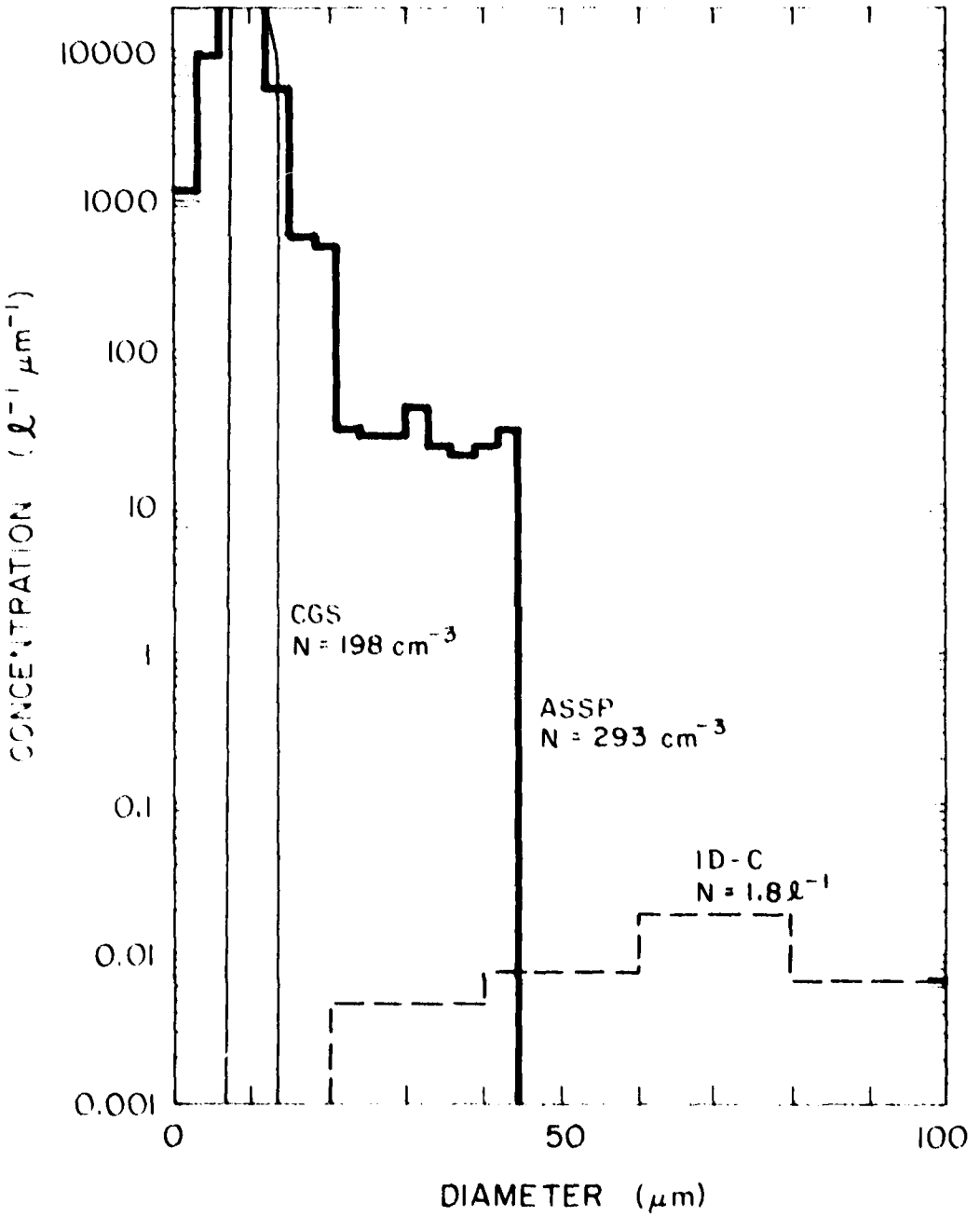

Figure 34. Concentration plotted against diameter for ice particles and water droplets sampled by the 1D-C probe (— —), the ASSP (———), and a cloud gun slide ( )exposed on 25 March 1979. The exposure was for 6.8 ms at 23212 MST; the 1D-C and ASSP data are 30 s averages around this time. "N" is the total ice particle or droplet concentration for each sample.

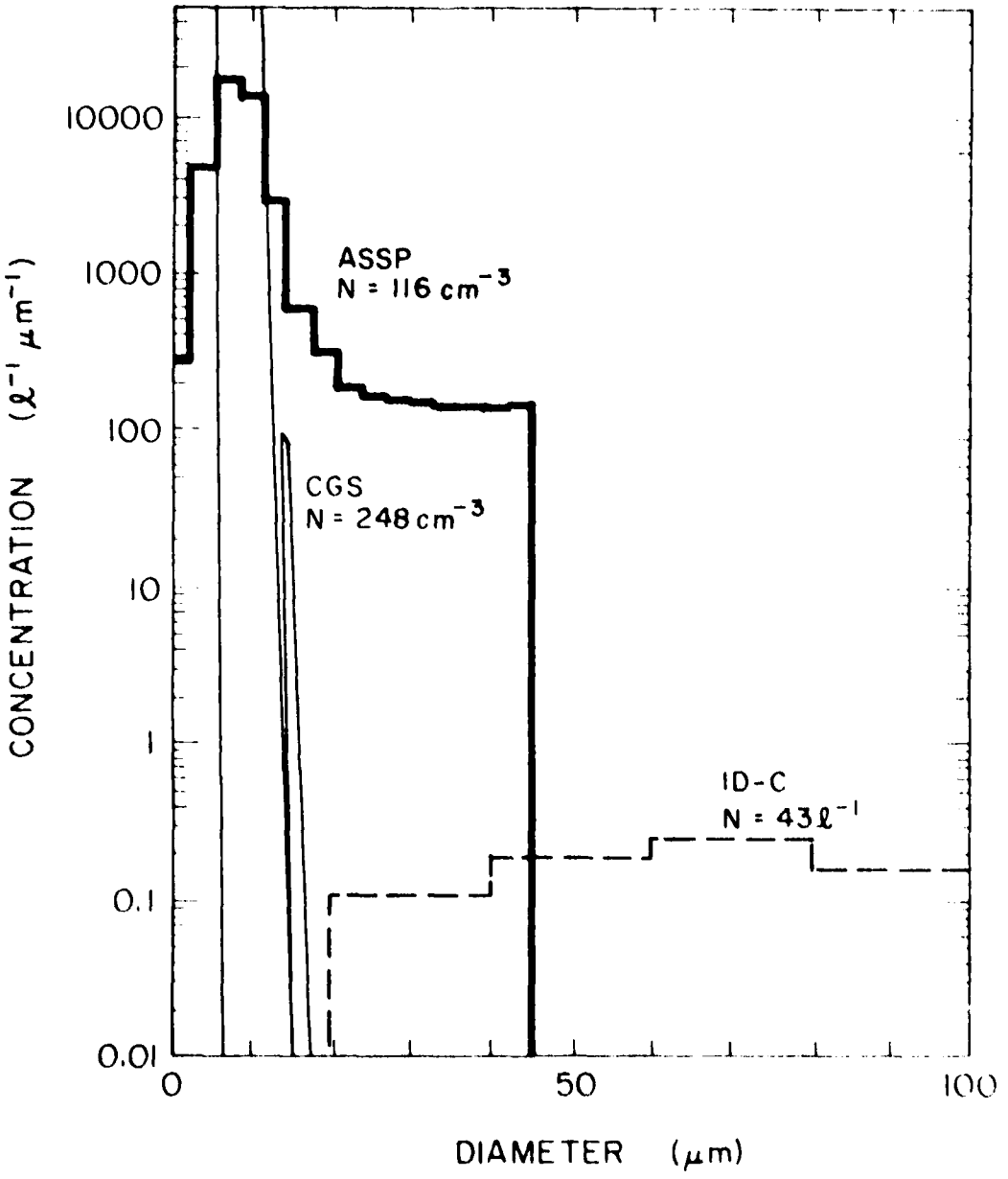

Figure 35 Concentration plotted against diameter for ice particles and water droplets sampled by the 1D-C probe (– – –), the ASSP (———), and a cloud gun slide (– · –) on 17 March 1979. The cloud gun slide was exposed for 4.2 ms at 09:51:5 MST, the 1D-C and ASSP samples are a 30 s average around that time. "N" is the total ice particle or droplet concentration for each sample.

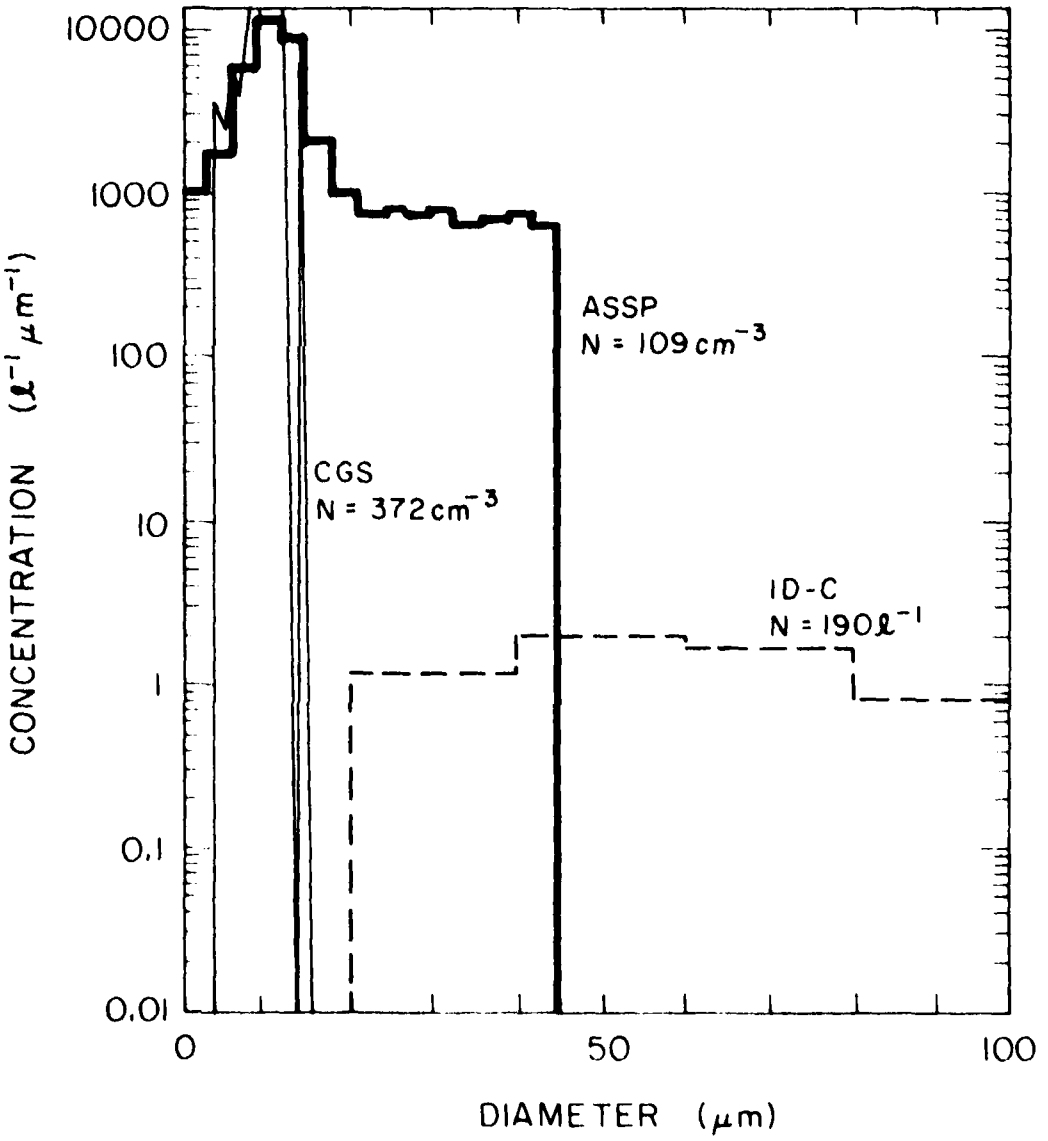

Figure 36 Concentration plotted against diameter for ice particles and water droplets sampled by the 1D-C probe (- - -), the ASSP (——) and a cloud gun slide (· · ·) on 4 April 1979. The cloud gun slide was exposed for 4.5 ms at 113552 MST, the 1D-C and ASSP samples are a 30 s average around that time. "N" is the total ice particle or droplet concentration for each sample.

A crystal can produce more than a single pulse if its size exceeds a limit (d_L) which is dependent on air velocity (TAS) and the reset time of the "strobe and reset" circuitry (Δt) $d_L = (TAS) \times (\Delta t)$. This size limit is: For TAS = 25 ms^{-1} and Δt = 5 ms, d_L = 125 μm; for TAS = 80 ms^{-1} and Δt = 5 ms, d_L = 400 μm. For the data on hand these limits were exceeded by many crystals. However, since the number of "false" pulses in many cases the number of crystals, it appears that unusual pulse shapes produced by scattering from crystals can result in multiple counts from each crystal, in a way not now understood. However, these flat distributions are easily distinguished from the spectra obtained from the cloud droplets at least when a broad distribution of cloud droplets is not encountered simultaneously.

5. SUMMARY AND CONCLUSIONS

From the studies discussed in this report we can derive the following preliminary conclusions concerning measurements of cloud particle spectra:

1. The measured sample area of the ASSP was found to be 0.35 mm^2 compared to the PMS value of 0.32 mm^2 and the velocity reject percentage was 68% compared to 62% given by PMS.

2. CGS and ASSP measured droplet spectra are in fairly close agreement, however, we suspect a sampling problem with the CGS as hinted at by the persistently high droplet concentrations it gives.

3. The response of the 2D-C probe at sizes > 100 μm is close to the PMS specifications, while counting efficiencies in the lower channels are somewhat higher than expected. There is as yet, however, no proof that the counts in these low channels are correctly interpreted.

4. The measured diameters of particles increase for particles further from the focal plane of the detector optics of the 2D-C and 1D-C probes. The overall effect of this is a slight oversizing of particles, ~ 25% at sizes near 100 μm, ~ 10% near 250 μm.

5. The 1D-C probe undercounts particles in the lower channels (< 140 μm) due to decreased depths of field for these small sizes. The depth of field corrections specified by PMS slightly overcorrect for this effect. The 1D-C probe also appears to undercount in higher channels (> 180 μm) and it is not known at this time whether this is due to mis-sizing or particle rejection.

6. The ASSP and FSSP probes respond to ice particles with a nearly uniform distribution of counts in all size channels. This flat spectrum is superimposed on any real droplet spectrum which may be present. The false counts are factors of 300 to 3000 higher than the actual concentrations of ice particles; the dependence of this factor on crystal type is not yet known.

The results obtained under this contract suggest several topics for study during the 1980 field season. These include:

1. Continuing bench determinations of depth of field for the FSSP and ASSP and velocity reject percentage for the ASSP in order to detect possible drifts in these values with time.

2. Development and testing of an improved cloud gun droplet sampler. This will be fashioned after the one currently used in our Queen Air research aircraft which has been shown to give satisfactory droplet spectra.

3. Laboratory and wind tunnel observations of the pulse shapes of the ASSP and FSSP, and comparison of their droplet spectra with those from the cloud gun.

4. Glass bead and water droplet tests on the 1D-C and 2D-C probes to determine the depths of field and counting efficiencies in the lower channels ($\sim$ 100 μm).

5. Further studies involving the 2D-C probe in comparison with data from impaction slides and the 1D-C probe in order to more closely study the response of ths probe to ice particles throughout its entire size spectrum.

6. Interpretation of the 2D-C depolarization data collected during the 1979 field season. Further studies of the 2D-C depolarization signal for different types of ice particles are also planned.

7. Investigation of the apparent undercounting of the 1D-C probe in the higher channels ($\tilde{>}$ 180 μm).

8. Explanation of the observed response of the ASSP and FSSP probes to ice particles.

REFERENCES

Knollenberg, R. G., 1975: "The response of optical array spectrometers to ice and snow: a study of probe size to crystal mass relationships". Air Force Cambridge Research Laboratories, Report No. AFCRL-TR-75-0494, September 1975.

Walsh, P. A., 1977: Cloud droplet measurements in wintertime clouds. M.S. Thesis, University of Wyoming, 170 pp.